Chapter 13

Aerodynamics of Wind Turbines

- 13.1 Introduction
  - Draw similarities between helicopter rotors and wind turbines
  - Classic analysis by Lock (1925)
  - More complicated than helicopter rotors
    - Ground boundary layers effects
    - Atmospheric turbulence
    - Wind gusts
    - Thermal convection stratification
    - Tower (another wind turbine) shadow
  - Classical blade element-momentum theory allows study of the effects of primary design variables (e.g. blade twist, planform, # of blades)

13.2 History

- First use in Babylonia times, Persians (7^{th} century), Europe (15^{th} century)
- 17^{th} century: Tower mills (twisted blades, tapered planforms control devices to point to the wind.
- 18^{th} century: Dutch bring wind mills to US; pumping water
- 20^{th} century: Used to generate power, especially in Europe.
- 2005: 2% of total energy demand (25GW)
- Typical configuration: HAWT: Horizontal Axis Wind Turbine; (lift machine) – see next figure; tall tower, alignment parallel to the wind, tower shadow 5-100m diameter (few KW-MW)
- VAWT: Vertical Axis Wind Turbine, not as common, less efficient, do not scale up easily
- Relative cost of wind energy still high, but going down

Figure 13.1 A modern three-bladed wind turbine. Source: Photo courtesy of Sandia National Laboratories.

Figure 13.2 Large wind turbines on a wind farm off the coast of Norway. Notice the large amount of bending on the blades, suggesting that they are operating at high thrust and generating maximum power. Source: Photo courtesy of Sandia National Laboratories.

13.3 Power in the Wind

- The kinetic energy per time through a disk of area A is

$$\frac{KE}{dt} = \frac{1}{2}\dot{m}|V_\infty|^2 = \frac{1}{2}\rho A|V_\infty|^3 = P \qquad (13.1)$$

if process is 100% efficient

- For example: d=5m, 50% efficient, velocity 10m/s standard see level

$$P = (0.5)\times\frac{1}{2}\rho A|V_\infty|^3 = 0.25\times 1.225\times(\pi 2.5^2)\times(10)^3 \approx 6\,\text{kW or } 8\,\text{hp} \qquad (13.2)$$

- It helps if diameter and wind speed are high
- If not perpendicular to wind velocity has $\cos\gamma$ factor, power drops by a $\cos^3\gamma$ factor

- 13.4 Momentum Theory Analysis for a Wind Turbine
  - Thrust not known; momentum theory alone is not enough, need BEMT

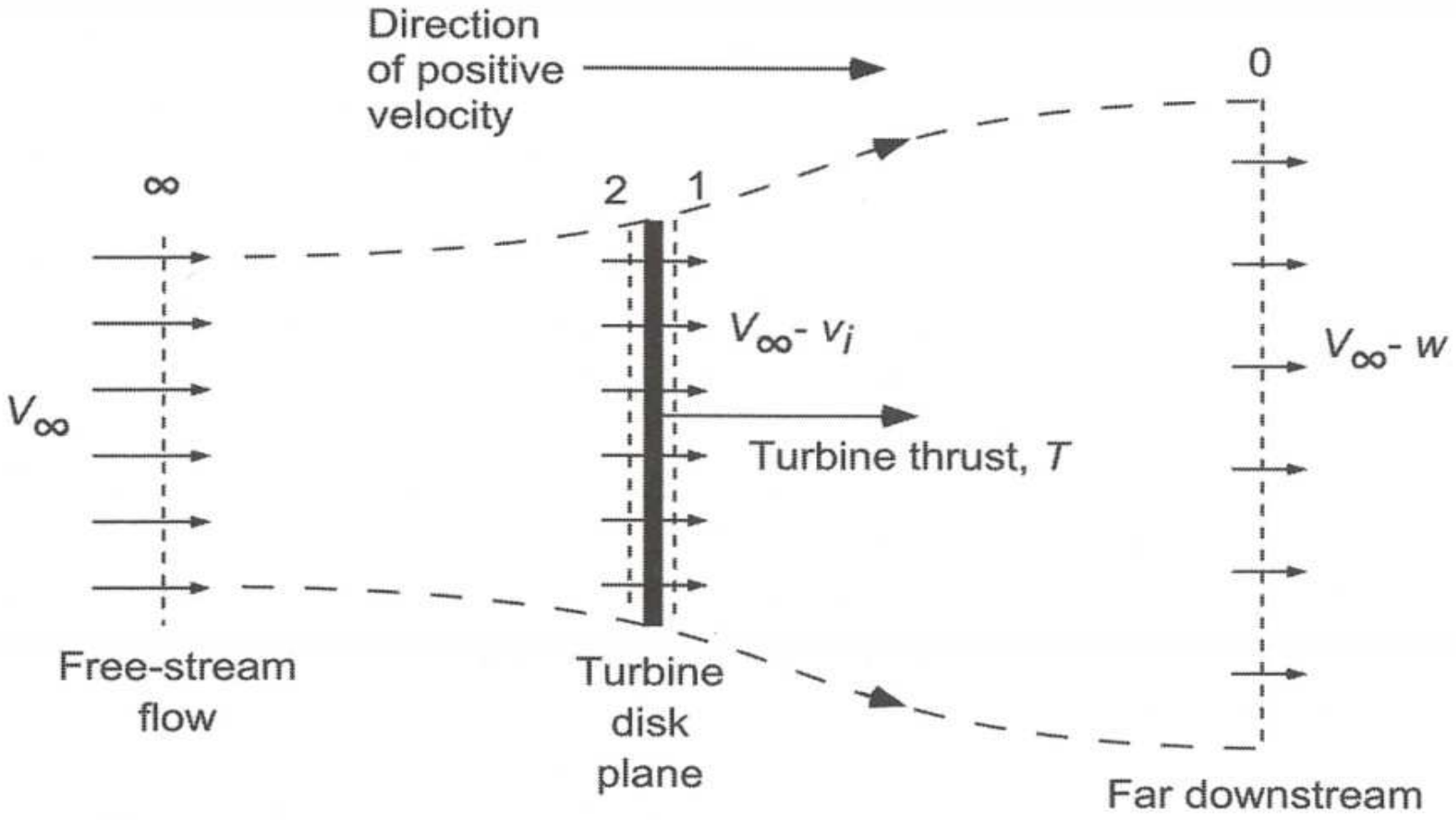

Figure 13.3 Flow model used for the momentum theory analysis of a wind turbine.

- Wind turbine extracts energy from the flow, thus velocity decreases, thus slipstream expands downstream
- Conservation of mass

$$\dot{m} = \rho A(V_\infty - v_i) \qquad (13.3)$$

- Change in momentum can be related to thrust

$$T = \dot{m}V_\infty - \dot{m}(V_\infty - w) \qquad (13.4)$$

- Expanding:

$$T = \dot{m}V_\infty - \dot{m}V_\infty + \dot{m}w = \dot{m}w \qquad (13.5)$$

- Work done on the air by the turbine per unit time is:

$$\dot{W} = \frac{1}{2}\dot{m}(V_\infty - w)^2 - \frac{1}{2}\dot{m}V_\infty^2 = \frac{1}{2}\dot{m}w(w - 2V_\infty) = -\frac{1}{2}\dot{m}w(2V_\infty - w) \qquad (13.6)$$

- Turbine does negative work (windmill state)
- Power:

$$P = T\,(V_\infty - v_i) = \frac{1}{2}\dot{m}w\,(2V_\infty - w) \qquad (13.7)$$

- Substituting 13.5 in 13.7:

$$T\,(V_\infty - v_i) = \frac{1}{2}\dot{m}w\,(2V_\infty - w) = \dot{m}w\,(V_\infty - v_i) \qquad (13.8)$$

- Thus $w=2\upsilon_i$ (or $\upsilon_i=w/2$); same as in helicopter rotors
- For model validity: $V_\infty - w > 0$; thus $V_\infty > w = 2\upsilon_i$

- Thrust not known; define induction ratio:
- $a=\upsilon_i/V$, or $\upsilon_i=aV$
- Larger a $\rightarrow$ more flow is slowed as it passes the turbine

- 13.4.1 Power and Thrust Coefficients
  - From 13.7 and 13.3

$$P = 2\rho A (V_\infty - v_i)^2 v_i \qquad (13.9)$$

  - Power coefficient (different from a helicopter)

$$C_P = \frac{P}{\frac{1}{2}\rho A V_\infty^3} \qquad (13.10)$$

  - Thus

$$C_P = \frac{2\rho A(V_\infty - v_i)^2 v_i}{\frac{1}{2}\rho A V_\infty^3} = \frac{4(V_\infty - v_i)^2 v_i}{V_\infty^3} = 4(1-a)^2 a \qquad (13.11)$$

  - Shown in following figure (valid for 0<a<1/2)

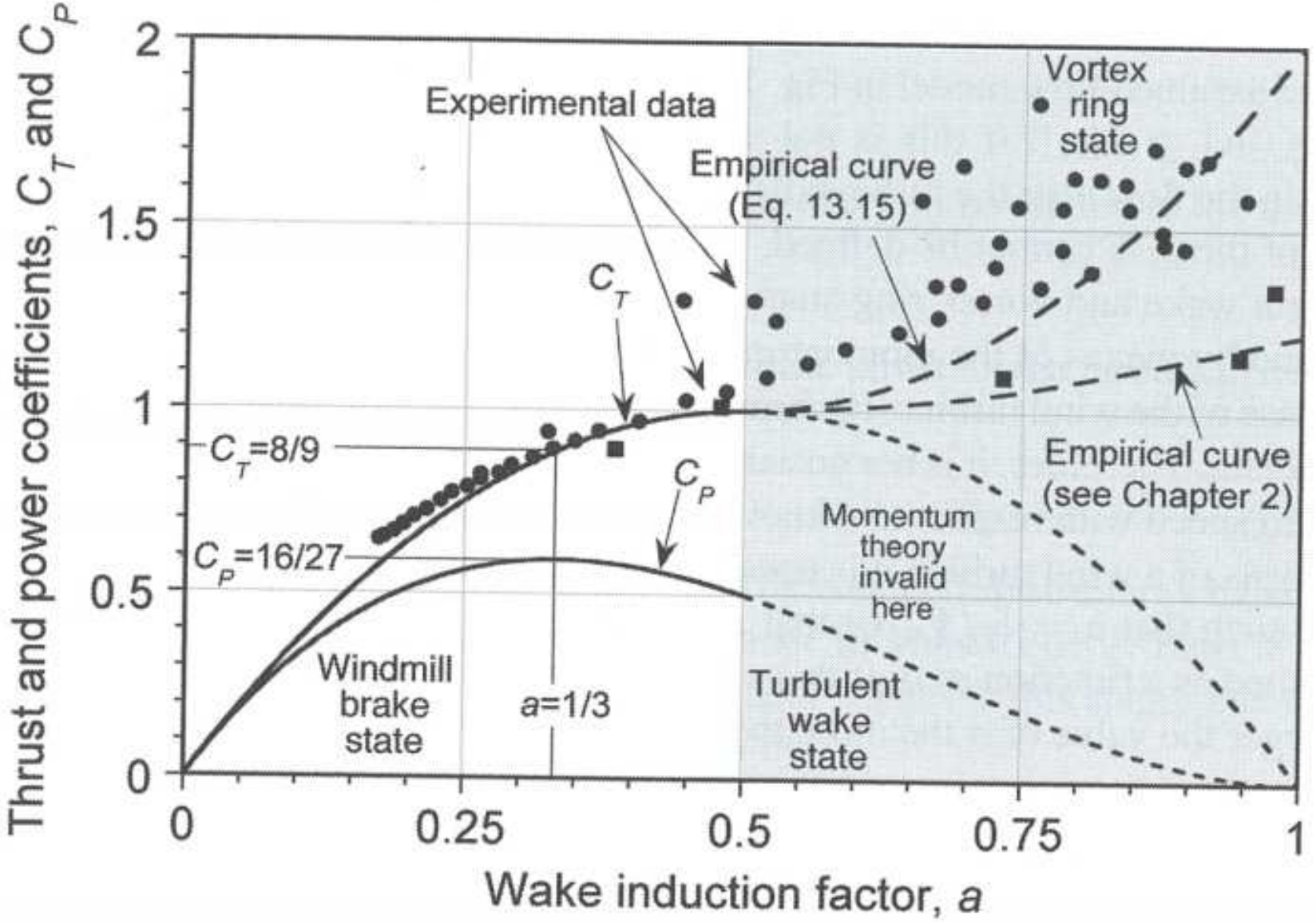

Figure 13.4 Momentum theory solution for a wind turbine in axial flow in terms of the induction ratio. Measurements from several sources including Lock (1925).

- For thrust using 13.3:

$$T = \dot{m}w = \rho A(V_\infty - v_i)w = 2\rho A(V_\infty - v_i)v_i \qquad (13.12)$$

- Thrust coefficient: $$C_T = \frac{T}{\frac{1}{2}\rho A V_\infty^2} \qquad (13.13)$$
- Using 13.12

$$C_T = \frac{2\rho A(V_\infty - v_i)v_i}{\frac{1}{2}\rho A V_\infty^2} = \frac{4(V_\infty - v_i)v_i}{V_\infty^2} = 4(1-a)a \qquad (13.14)$$

- Empirical results for a>0.5 are shown; e.g.

$$C_T = 4(a-1)a + 2 \qquad (13.15)$$

- Note that:

$$C_T = 4\left(\frac{V_c}{v_h}\right)^{-2} \quad \text{and} \quad a = \frac{v_i}{V_c} = \frac{v_i}{v_h}\left(\frac{V_c}{v_h}\right)^{-1} \qquad (13.16)$$

13.4.2 Theoretical Maximum Efficiency

- Differentiate 13.11 wrt a

$$\frac{dC_p}{da} = 4(1 - 4a + 3a^2) = 0 \qquad (13.17)$$

- Thus

$$a = \frac{1}{3}, \quad C_T = \frac{8}{9} = 0.89 \text{ and } C_P = \frac{16}{27} = 0.59 \qquad (13.18)$$

- Betz-Lanchester limit; upper limit for power extraction
  - No viscous or other losses
  - Typically: C_P = 0.4 – 0.5 (66-83% of max)

- 13.5 Representative Power Curve
  - See following figure for 47m/0.66MW turbine
    - “cut-in” speed to overcome friction
    - Rated power – to make sure power can be absorbed by electric generator
      - Blade pitch control (stall at high speeds)
      - Furling (mechanical/aerodynamic brake)

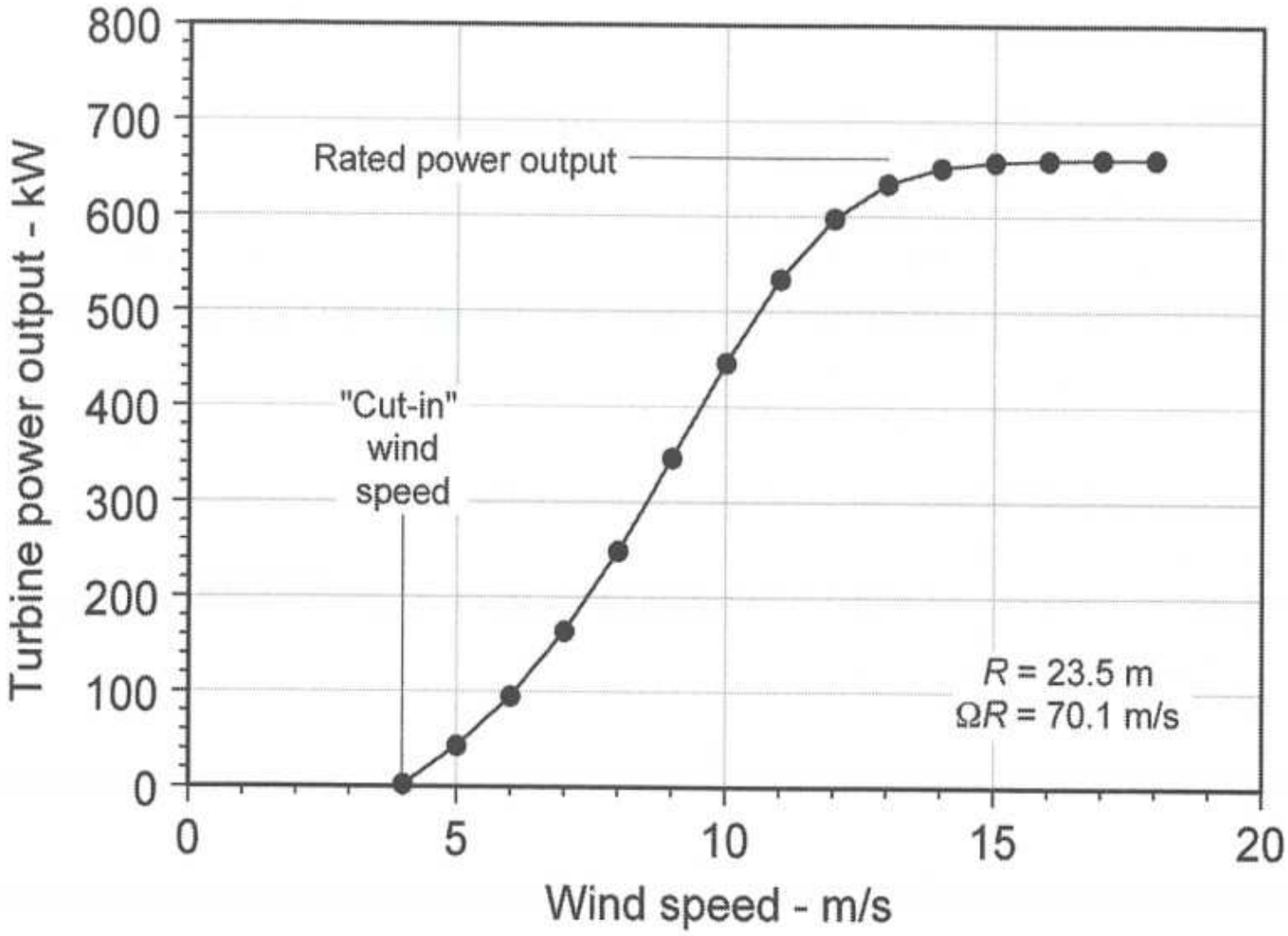

Figure 13.5 Power output from a representative constant tip-speed wind turbine as a function of wind speed.

- Define tip speed ratio (TSP)

  (similar to advance ratio μ for helicopter rotors)

$$X_{\text{TSR}} = \frac{\text{turbine tip speed}}{\text{wind speed}} = \frac{\Omega R}{V_\infty} \qquad (13.19)$$

- The corresponding C_P is shown in the next figure
  - Peak efficiency only at a fixed value of wind speed
- Another option is a variable speed turbine (more common today) – see figure
  - More efficient extraction at low speeds
  - Lower efficiency at high speeds

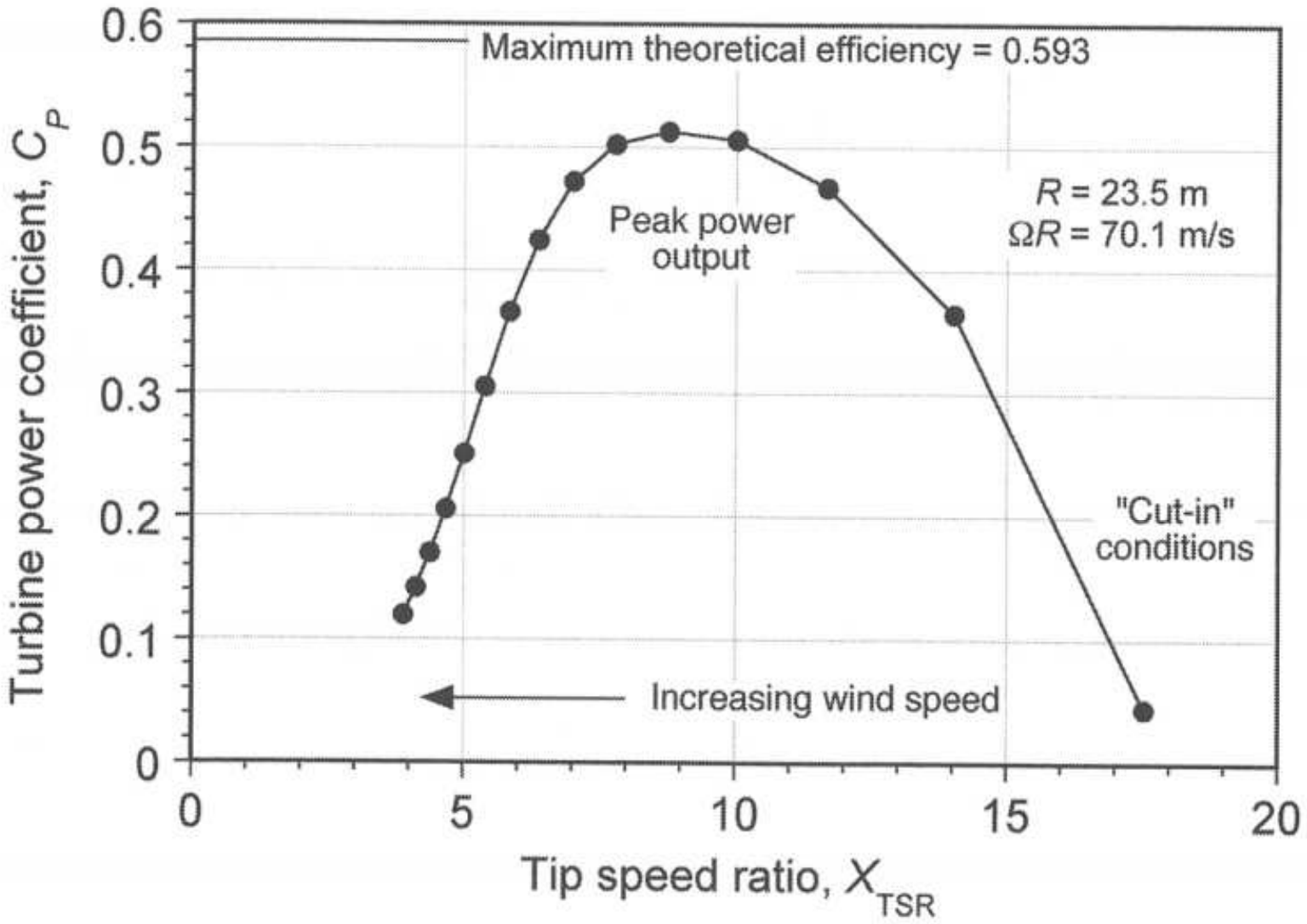

Figure 13.6 Representative power coefficient versus tip-speed ratio curve for a constant speed (rpm) horizontal axis wind turbine.

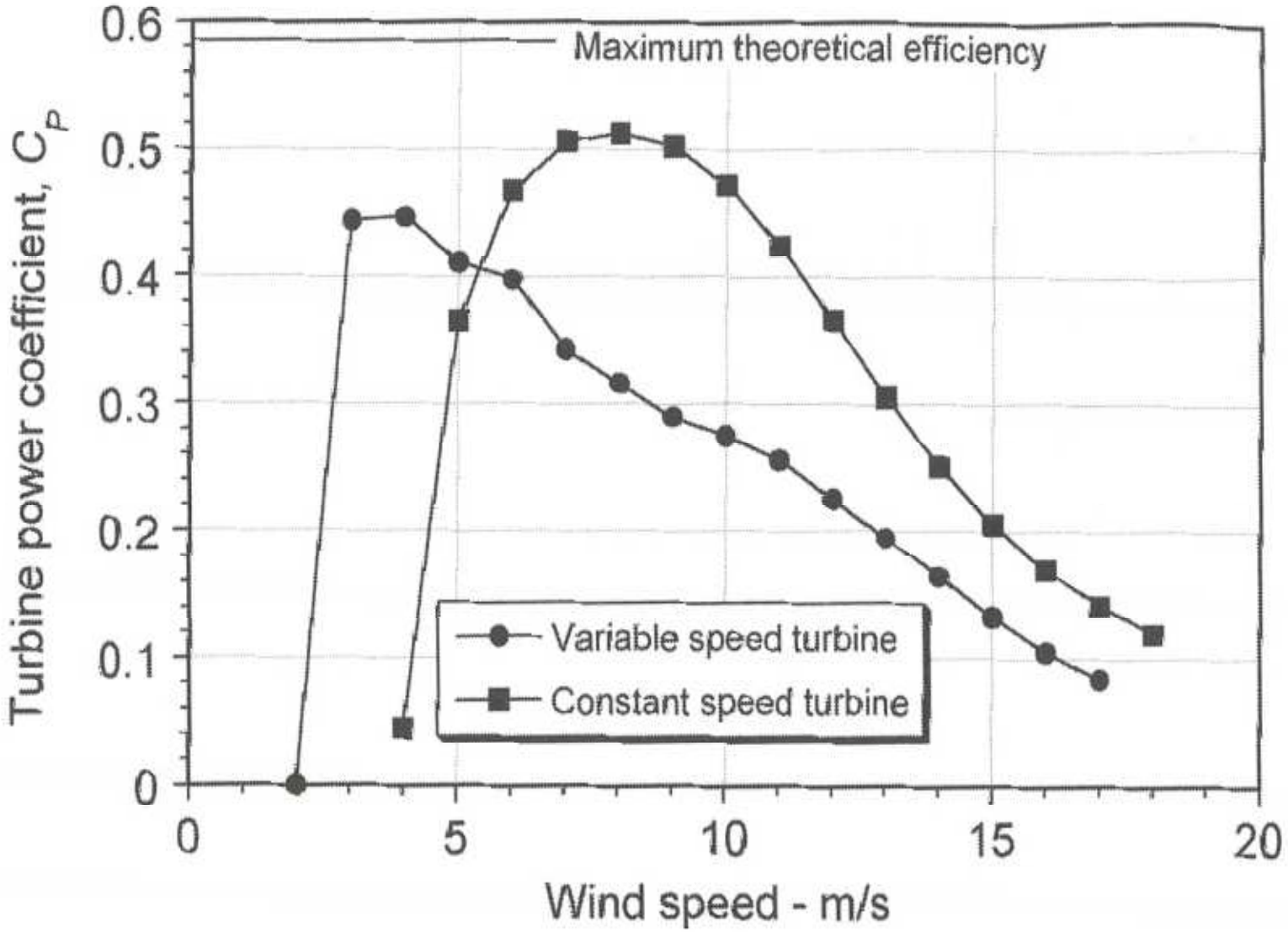

Figure 13.7 Representative power coefficient versus wind speed curves for constant speed and variable speed types of horizontal axis wind turbines.

13.6 Elementary Wind Models

- Factors affecting power: wind speed, tower height, likelihood of gusts
  - Standard atmosphere (section 5.2)

- For height
  - Power law

$$V_\infty(h) = V_\infty(h_{\text{ref}}) \left(\frac{h}{h_{\text{ref}}} \right)^m \qquad (13.20)$$

h_{ref}=10m, m=1/6 or 1/7

  - Logarithmic law

$$V_\infty(h) = V_\infty(h_{\text{ref}}) \left(\frac{\ln(h/z_0)}{\ln(h_{\text{ref}}/z_0)} \right) \qquad (13.21)$$

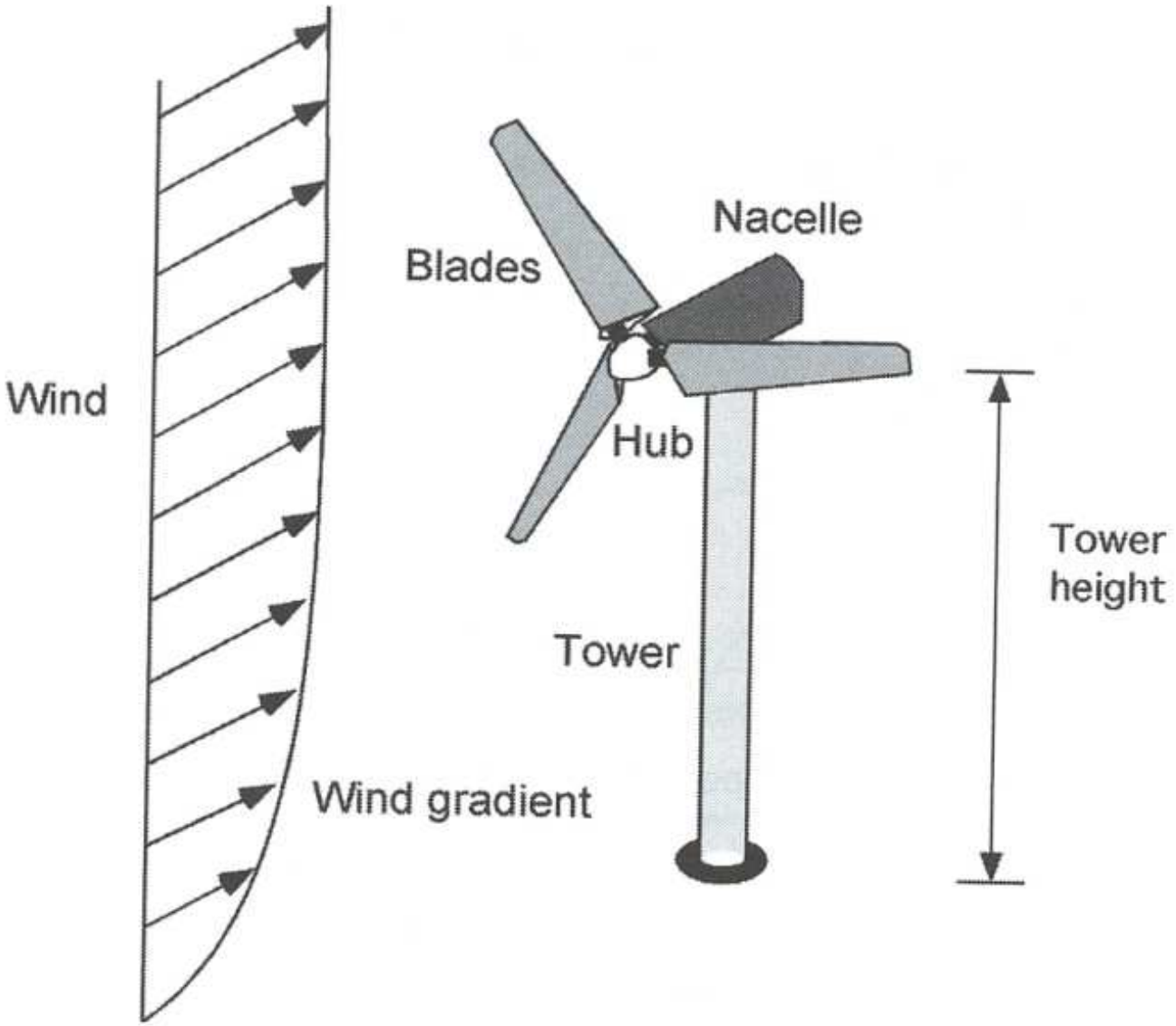

Figure 13.8 A wind turbine operates in an atmospheric boundary layer.

zo values:

Table 13.1. *Coefficients of Logarithmic Atmospheric Boundary Layer Model*

Type of terrain	z_0 (m)	m
Open country	0.02	0.12
Rural with few trees	0.05	0.16
Rural with trees and towns	0.3	0.928
Open water	0.001	0.01

- Stochastic variations of speed

$$V_\infty(t) = \bar{U} + u(t) \qquad (13.22)$$

- Turbulence intensity I_u

$$I_u = \frac{1}{\bar{U}} \left[\int_0^T u(t)^2 dt \right]^{1/2} \qquad (13.23)$$

  - T=time interval (e.g. 10secs)
  - I_u : 0.1U-0.2U, function of h, larger at low wind speeds
- Average power generated (probability distribution p(V)

$$\bar{P} = \int_0^\infty P(V_\infty) p(V_\infty)\, dV_\infty \qquad (13.24)$$

$$\text{Capacity factor} = \frac{\bar{P}}{\text{Rated power}} \qquad (13.25)$$

- Good wind models are needed

13.7 Blade Element Model for the Wind Turbine

- Similar to helicopter rotor in descend
- Angle of attack $\alpha=\theta+\phi$
- Assume swirl components are low
- Incremental lift and drag are

$$dL = \frac{1}{2}\rho U^2 c C_l \, dy \quad \text{and} \quad dD = \frac{1}{2}\rho U^2 c C_d \, dy \tag{13.26}$$

- Perpendicular and parallel to the rotor disk:

$$dF_z = dL\cos\phi + dD\sin\phi \quad \text{and} \quad dF_x = dL\sin\phi - dD\cos\phi \tag{13.27}$$

- Contributions to thrust, torque, power

$$dT = N_b \, dF_z, \quad dQ = N_b y \, dF_x \quad \text{and} \quad dP = N_b \Omega y \, dF_x \tag{13.28}$$

- If precone angle multiply thrust by $\cos\beta_p$

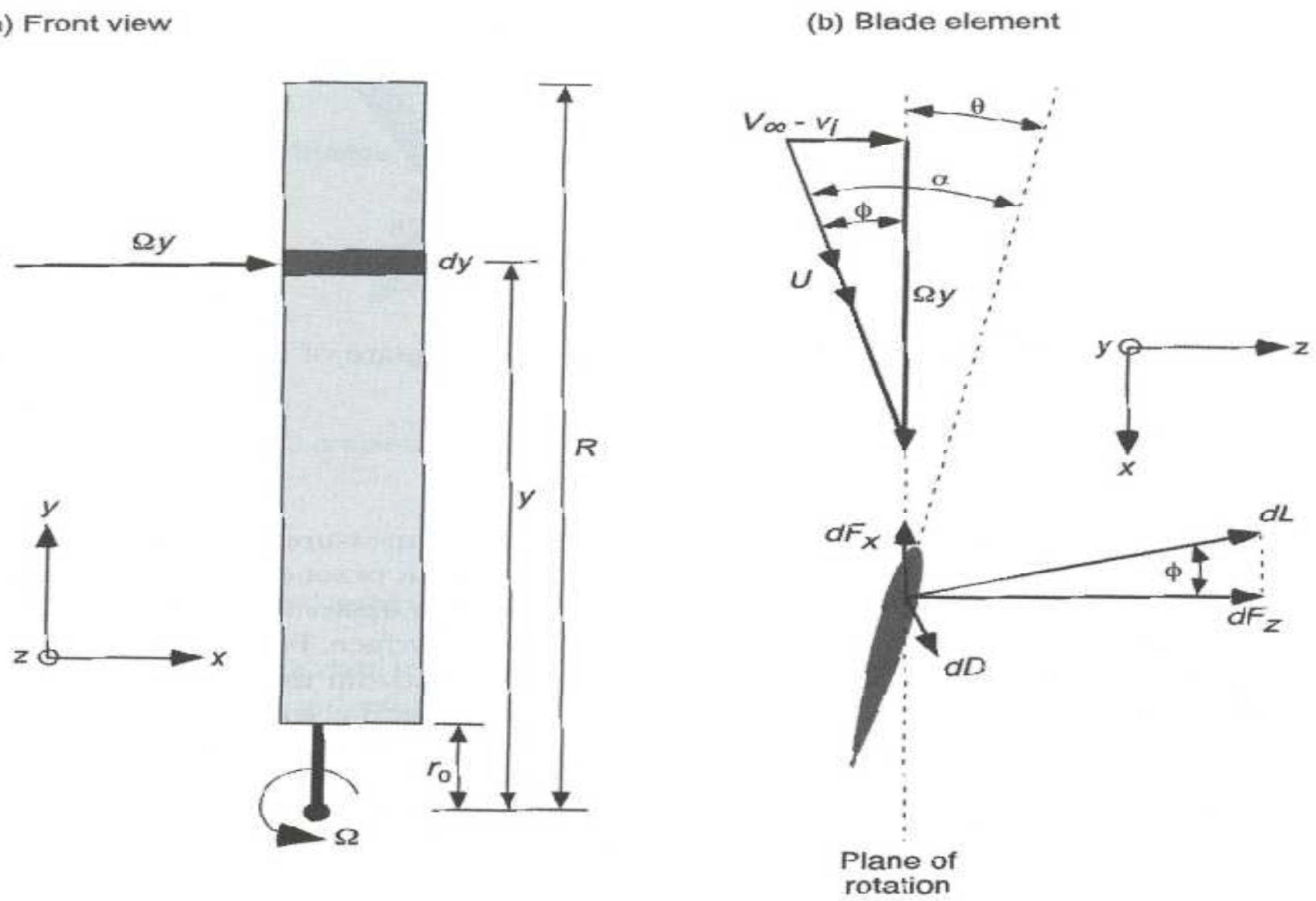

Figure 13.9 Blade element model for a wind turbine operating in axial (unyawed) flow.

- Substituting expresions from13.27

$$dT = N_b(dL\cos\phi + dD\sin\phi) \tag{13.29}$$

$$dQ = N_b(dL\sin\phi - dD\cos\phi)y \tag{13.30}$$

$$dP = N_b(dL\sin\phi - dD\cos\phi)\Omega y \tag{13.31}$$

- Assuming small angles:

$$dT = N_b(dL + \phi dD) \tag{13.32}$$

$$dQ = N_b(\phi dL - dD)y \tag{13.33}$$

$$dP = N_b\Omega(\phi dL - dD)y \tag{13.34}$$

- Nondimensionalizing:

$$dC_T = \frac{N_b dL}{\frac{1}{2}\rho A V_\infty^2} = \frac{N_b(\frac{1}{2}\rho(\Omega y)^2 c(C_l + \phi C_d)\,dy)}{\frac{1}{2}\rho(\pi R^2)V_\infty^2} \tag{13.35}$$

$$= \left(\frac{N_b c}{\pi R}\right)\left(\frac{\Omega y}{V_\infty}\right)^2 (C_l + \phi C_d)\,dr = \sigma X^2(C_l + \phi C_d)\,dr \tag{13.36}$$

- Where $r=y/R$, $\sigma=N_b c/\pi R$, as before
- $X=\Omega y/V_\infty$ local section speed ratio

$$X = \frac{\Omega y}{V_\infty} = \frac{\Omega R}{V_\infty}\left(\frac{\Omega y}{\Omega R}\right) = X_{\text{TSR}} r \qquad (13.37)$$

- Thrust coefficient

$$dC_T = \sigma X_{\text{TSR}}^2 (C_l + \phi C_d) r^2 \, dr \qquad (13.38)$$

- Power coefficient

$$dC_P = \sigma X_{\text{TSR}}^3 (\phi C_l - C_d) r^3 \, dr \qquad (13.39)$$

- Inflow angle

$$\phi = \tan^{-1}\left(\frac{V_\infty - v_i}{\Omega y}\right) \approx \frac{V_\infty - v_i}{\Omega y} = \left(\frac{V_\infty - a V_\infty}{\Omega R}\right)\left(\frac{\Omega R}{\Omega y}\right) = \left(\frac{1-a}{r X_{\text{TSR}}}\right) \qquad (13.40)$$

- To evaluate C_T and C_P need υ_i and local C_l C_d, $a=a(V,\theta,\upsilon_i)$
- 2D lift drag coefficients can be assumed
- Similar to helicopters (sec. 3.3)

13.8 Blade Element Momentum Theory

- BEMT a hybrid method - BEM plus momentum on annuli (use 2D lift/drag) - allows evaluation of the induction factor
- Works OK when wind perpendicular turbine blade
- Allows understanding of the effects of geometric parameters
- Similar to helicopters (section 3.2)
- Mass flow on annulus of turbine disk

$$d\dot{m} = \rho dA(V_\infty - v_i) = 2\pi\rho(V_\infty - v_i)y\,dy \qquad (13.41)$$

- Using differential form of 13.12:

$$dT = 2\rho(V_\infty - v_i)v_i dA = 4\pi\rho(V_\infty - v_i)v_i y\,dy \qquad (13.42)$$

- Non-dimensionalizing:

- Non-dimensionalizing:

$$dC_T = 8\left(1 - \frac{v_i}{V_\infty}\right)\frac{v_i}{V_\infty} r\, dr = 8(1-a)ar\, dr \qquad (13.43)$$

- This integrates to 13.14
- Using 13.38

$$dC_T = 8(1-a)ar\, dr = \sigma X_{\text{TSR}}^2 (C_l + \phi C_d) r^2\, dr \qquad (13.44)$$

- The second term is small:

$$dC_T = \sigma X_{\text{TSR}}^2 C_l r^2\, dr \qquad (13.45)$$

- Assuming no stall

$$C_l = C_{l_\alpha}(\theta - \alpha_0 + \phi) \quad \text{with} \quad \phi = \left(\frac{1-a}{r X_{\text{TSR}}}\right) \qquad (13.46)$$

- The lift coefficient becomes:

$$C_l = C_{l_\alpha}\left(\theta - \alpha_0 + \frac{1-a}{rX_{\text{TSR}}}\right) \tag{13.47}$$

- Using this (and assuming α_0 can be absorbed into θ)

$$8(1-a)a = \sigma X_{\text{TSR}}^2 C_l r = \sigma X_{\text{TSR}} C_{l_\alpha}\left(X_{\text{TSR}}\theta r + (1-a)\right) \tag{13.48}$$

- After some algebra

$$a^2 - \left(\frac{\sigma X_{\text{TSR}} C_{l_\alpha}}{8} + 1\right)a + \frac{\sigma X_{\text{TSR}} C_{l_\alpha}(X_{\text{TSR}}\theta r + 1)}{8} = 0 \tag{13.49}$$

- Thus:

$$a(r, X_{\text{TSR}}) = -\sqrt{\left(\frac{\sigma X_{\text{TSR}} C_{l_\alpha}}{16} + \frac{1}{2}\right)^2 - \frac{\sigma X_{\text{TSR}} C_{l_\alpha}(X_{\text{TSR}}\theta r + 1)}{8}} + \left(\frac{\sigma X_{\text{TSR}} C_{l_\alpha}}{16} + \frac{1}{2}\right). \tag{13.50}$$

- Fundamental equation of BEMT allows calculation of a and vi as a function of r for a given blade pitch, twist, chord, airfoil section ($C_{l\alpha}$, a_o)
- Similarity with eq. 3.61 (climbing rotor)
- $C_{l\alpha}$ can be approximated with 2π; valid when $0<a<0.5$
- Rotor thrust and power can be found by integration:

$$C_T = \sigma X_{\text{TSR}}^2 \int_0^1 C_l r^2 \, dr \quad \text{or} \quad C_T = 8 \int_0^1 (1-a) a r \, dr \tag{13.51}$$

$$C_P = \sigma X_{\text{TSR}}^3 \int_0^1 (\phi C_l - C_d) r^3 \, dr \tag{13.52}$$

- Power can be expanded

$$C_P = \sigma X_{\text{TSR}}^3 \int_0^1 \phi C_l r^3 \, dr - \sigma X_{\text{TSR}}^3 \int_0^1 C_d r^3 \, dr \tag{13.53}$$

- In the ideal case a is uniform, and $C_d = C_{do}$

- In the ideal case a is uniform, and $C_d=C_{do}$

$$C_P = \sigma X_{\text{TSR}}^3 \int_0^1 \phi C_l r^3 \, dr - \sigma X_{\text{TSR}}^3 \int_0^1 C_d r^3 \, dr$$
$$= X_{\text{TSR}} \int_0^1 dC_T \phi r dr - \sigma X_{\text{TSR}}^3 \int_0^1 C_{d_0} r^3 \, dr$$
$$= C_T(1-a) + \frac{\sigma X_{\text{TSR}}}{4} C_{d_0}, \qquad (13.54)$$

- The first term is the induced power from simple momentum theory
- Second term (profile power) depends on σ, C_d, tip speed
- Eq. 13.50: For uniform a; θr=constant, ideal twist (section 3.3.3); lowest induced losses on the turbine.
  - Magnitude of twist depends on tip velocity (figs 13.10-13.11) – a low blade pitch works for a wide range of wind speeds
- a=1/3 condition for max energy (valid for 0<a<0.5)

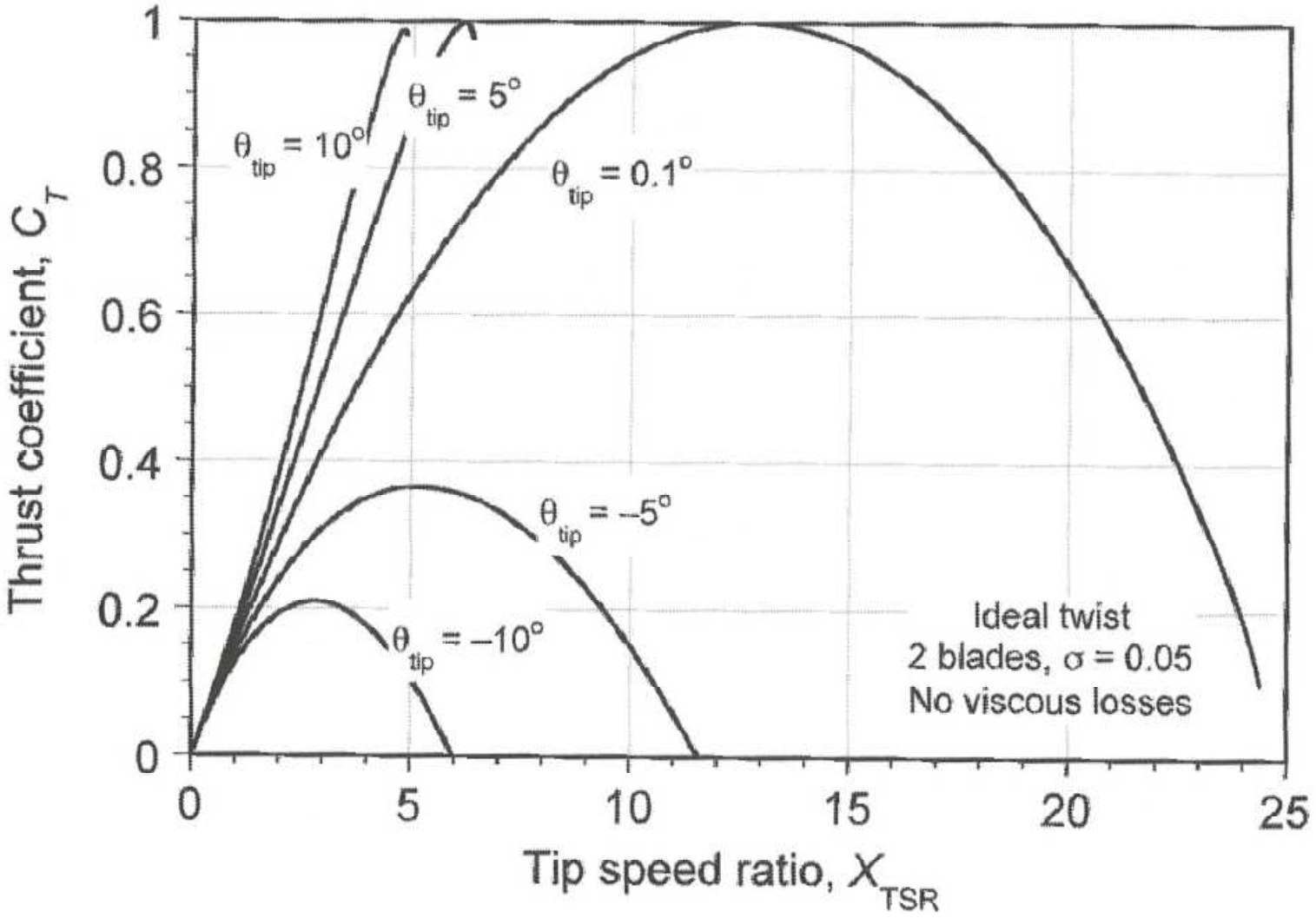

Figure 13.10 Representative thrust produced on a wind turbine as a function of tip speed ratio using the BEMT for various pitch angles. No nonideal losses.

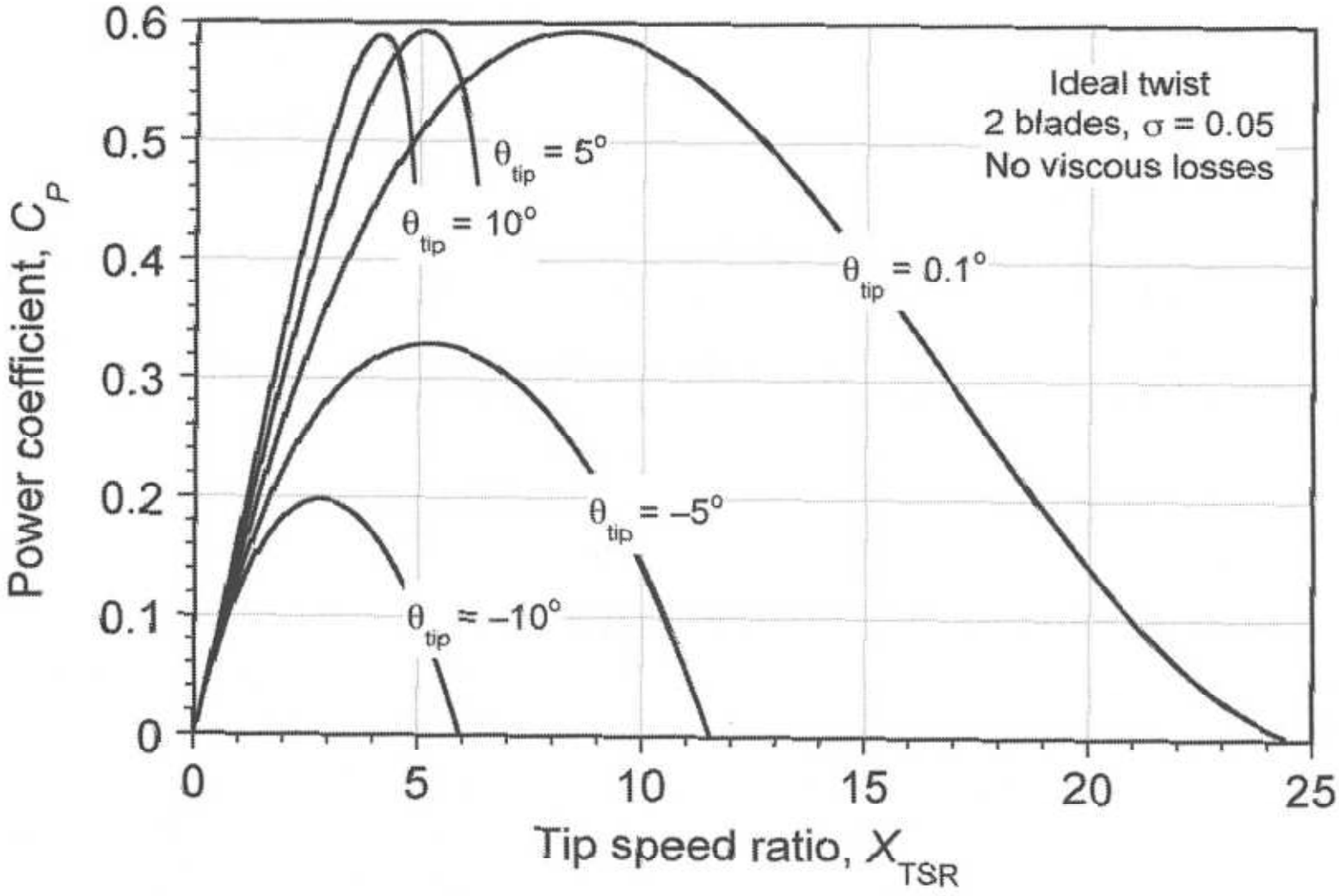

Figure 13.11 Representative power output produced from a wind turbine as a function of tip speed ratio using the BEMT for various pitch angles. No nonideal losses.

- 13.8.1 Effect of the number of blades
  - See fig 13.12
  - Increasing Nb (or s) does not affect max efficiency
  - Affects tip speed ratio where maximum efficiency is obtained

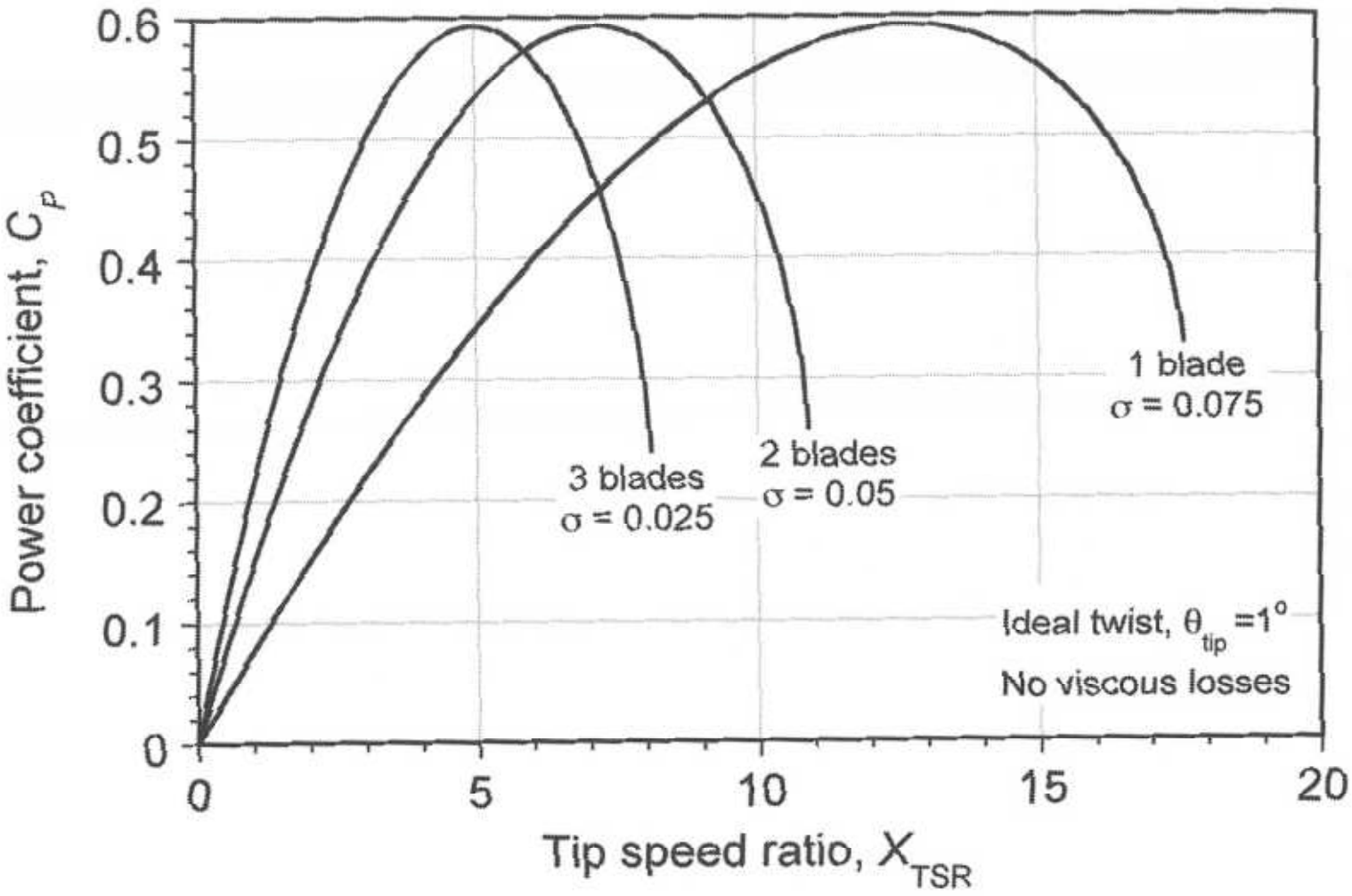

Figure 13.12 Representative power output produced from a wind turbine for different numbers of blades as a function of tip speed ratio using the BEMT. No nonideal losses.

- 13.8.2 Effect of Viscous Drag
  - See fig. 13.13
  - Lower drag → higher maximum efficiency
  - Usually $0.01 \leq C_{do} \leq 0.02$

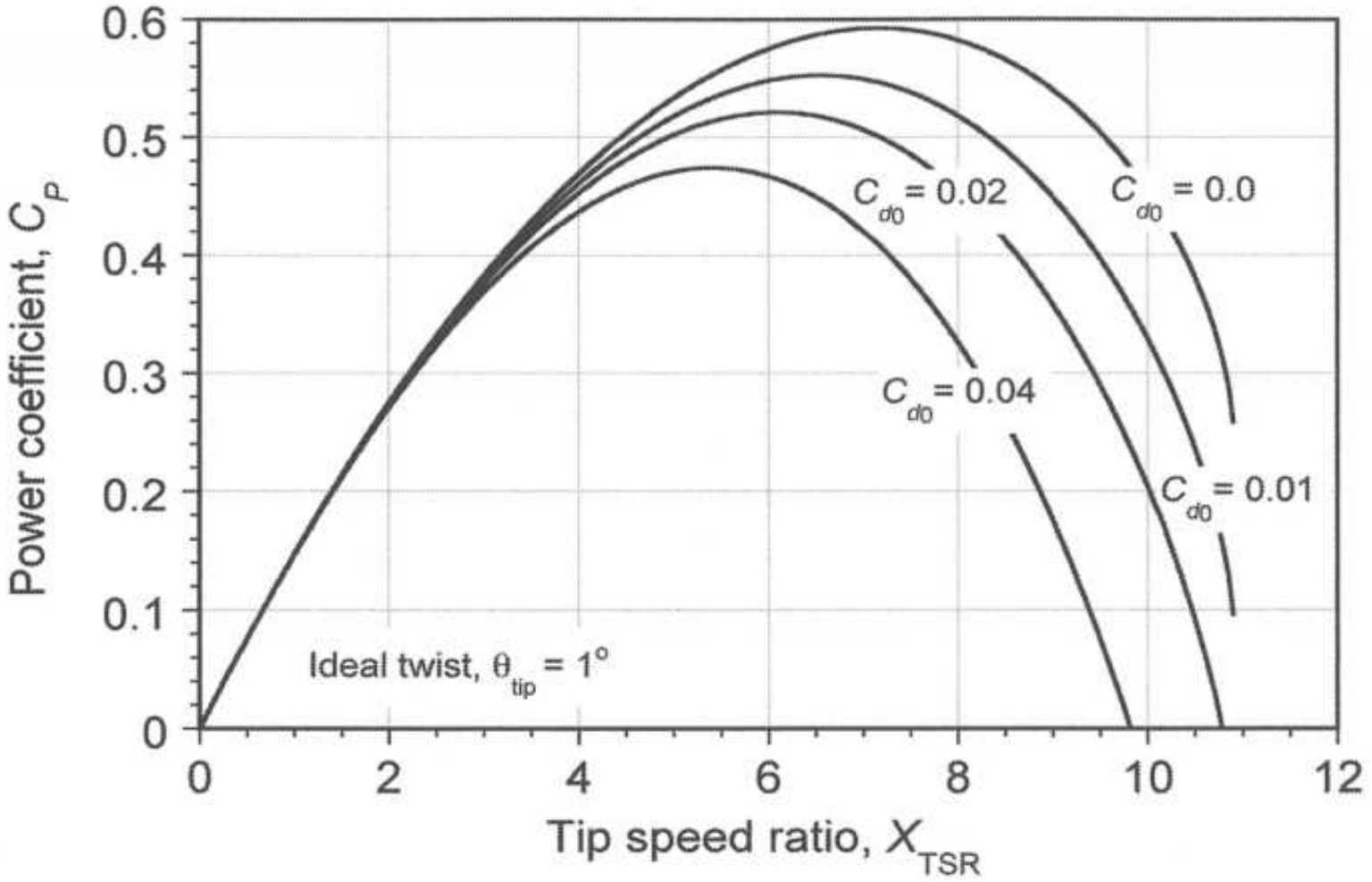

Figure 13.13 Representative power output from a wind turbine for airfoil sections with different assumed viscous drag coefficients as a function of tip speed ratio using the BEMT. No tip losses.

13.8.3 Tip-Loss Effects

- Prandtl's "tip-loss" correction factor F (section 3.3.10)

$$dC_T = 8F(1-a)ar\,dr \quad \text{where} \quad F = \left(\frac{2}{\pi}\right)\arccos\left(\exp(-f)\right) \tag{13.55}$$

- Where f:

$$f = \frac{N_b}{2}\left(\frac{1-r}{r\phi}\right) = \frac{N_b}{2}\left(\frac{1-r}{1-a}\right)X_{\text{TSR}} \tag{13.56}$$

- If root is included:

$$f = \frac{N_b}{2}\left(\frac{r-r_0}{1-a}\right)X_{\text{TSR}} \tag{13.57}$$

- Put into eq. 13.50 (BEMT)

$$a(r, X_{\text{TSR}}, F) = -\sqrt{\left(\frac{\sigma X_{\text{TSR}} C_{l_\alpha}}{16F} + \frac{1}{2}\right)^2 - \frac{\sigma X_{\text{TSR}} C_{l_\alpha}(X_{\text{TSR}}\theta r + 1)}{8F}} + \left(\frac{\sigma X_{\text{TSR}} C_{l_\alpha}}{16F} + \frac{1}{2}\right). \tag{13.58}$$

- Iterations: assume F=1 initially, calculate a and F from eqs 13.58 and 13.55; 3-10 iterations
- From 13.58 sqrt needs to be positive

$$\left(\frac{\sigma X_{\text{TSR}} C_{l_\alpha}(X_{\text{TSR}}\theta r + 1)}{8F}\right) > \left(\frac{\sigma X_{\text{TSR}} C_{l_\alpha}}{16F} + \frac{1}{2}\right)^2 \qquad (13.59)$$

- F limits the range of wind speeds and operating conditions f
- If a > 0.5 eq. 13.15 can be used (empirical)
- Equating momentum and blade element:

$$(8(a-1)a + 4)\,F = \sigma X_{\text{TSR}}^2 C_l r = \sigma X_{\text{TSR}} C_{l_\alpha}\left(X_{\text{TSR}}\theta r + (1-a)\right) \qquad (13.60)$$

- After some algebra:

$$a^2 + \left(\frac{\sigma X_{\text{TSR}} C_{l_\alpha}}{8F} - 1\right)a + \left(\frac{1}{2} - \frac{\sigma X_{\text{TSR}} C_{l_\alpha}(X_{\text{TSR}}\theta r + 1)}{8F}\right) = 0 \qquad (13.61)$$

- Solution:

$$a(r, X_{\text{TSR}}, F) = \sqrt{\left(\frac{\sigma X_{\text{TSR}} C_{l_\alpha}}{16F} - \frac{1}{2}\right)^2 - \left(\frac{1}{2} - \frac{\sigma X_{\text{TSR}} C_{l_\alpha} (X_{\text{TSR}} \theta r + 1)}{8F}\right)} - \left(\frac{\sigma X_{\text{TSR}} C_{l_\alpha}}{16F} - \frac{1}{2}\right) \quad (13.62)$$

- Valid for $0.5 < a \leq 1.0$
- OK for engineering purposes
- Representative solutions are shown in figure 13.14

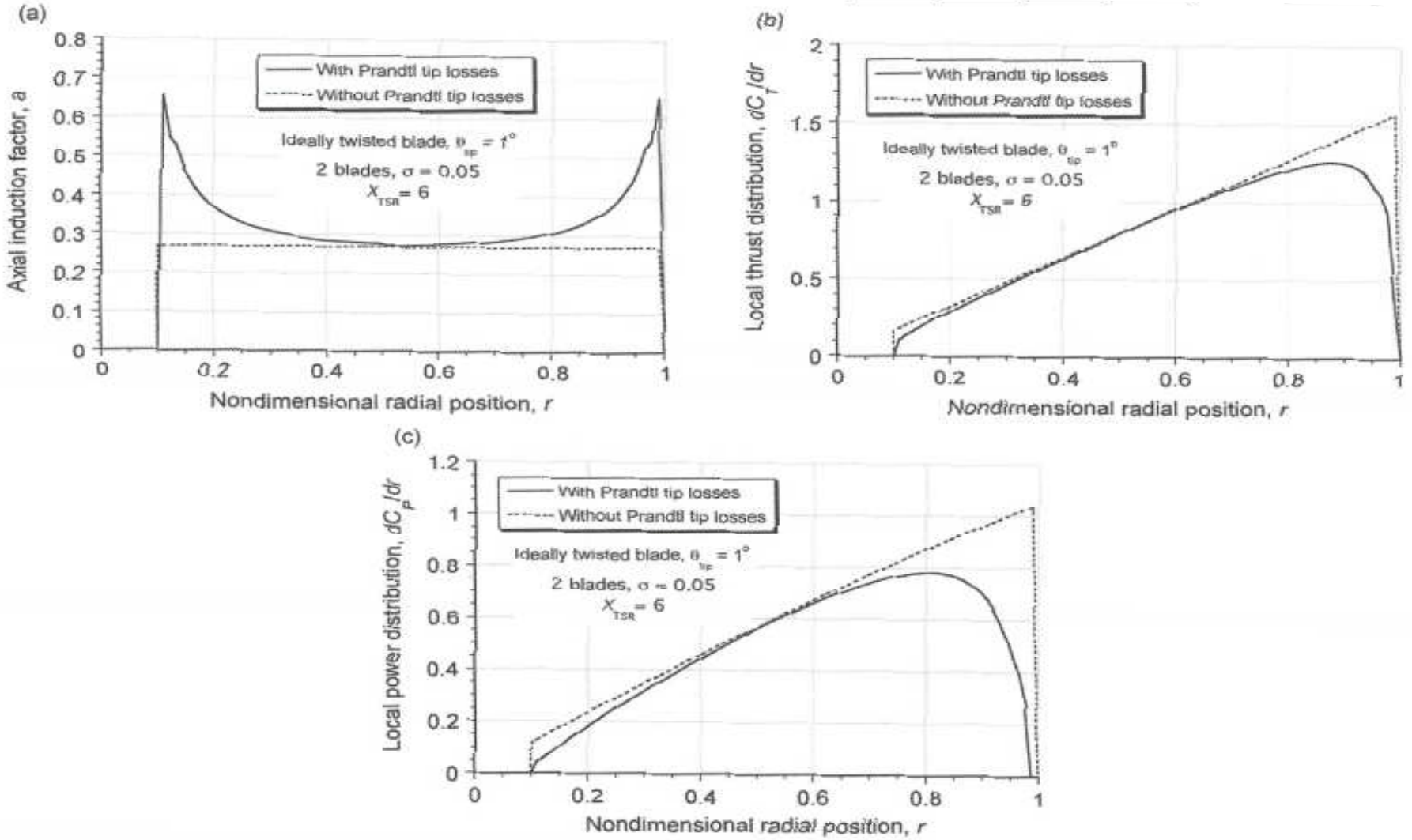

Figure 13.14 Representative distributions of induction ratio, thrust loading and torque loading for a wind turbine using ideal twist with and without Prandtl tip-loss effects. $X_{TSR} = 6$, $\sigma = 0.05$, $\theta_{tip} = 1°$, $r_0 = 0.1$ (a) Induction ratio. (b) Thrust distribution. (c) Power extraction distribution.

13.8.4 Tip Losses and Other Viscous Losses

- Fig. 13.15 shows effects of tip losses and viscous losses – decrease power by 15%

- Fig 13.16 shows the axial induction factor as a function of tip speed ratio for several blade pitch angles.
  - Larger a at high X
  - At low wind speeds possibility of two directions (empirical relationship between Ct and a)
  - At high wind speeds possible stall

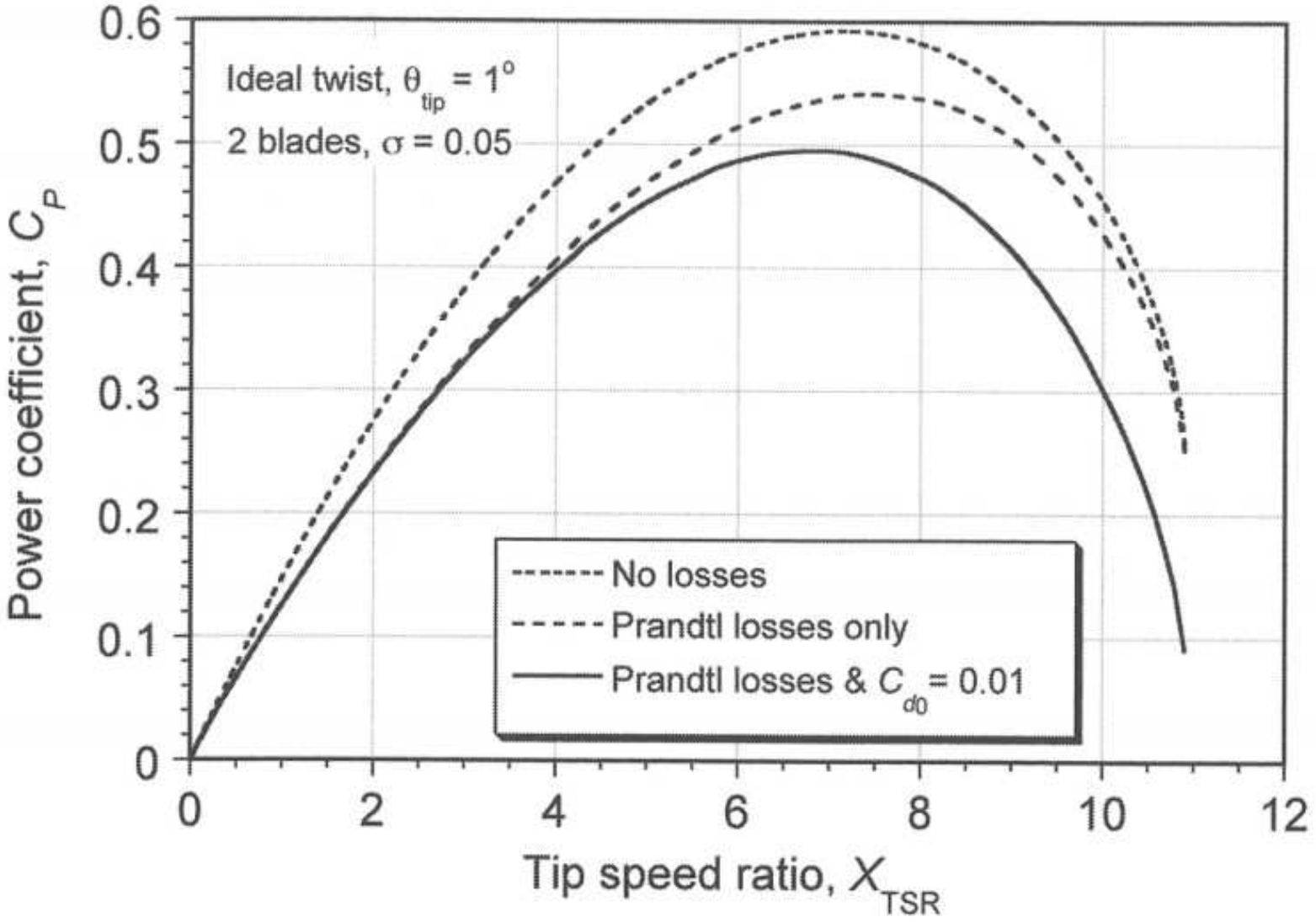

Figure 13.15 Turbine power output as a function of TSR showing the separate effects of viscous drag and Prandtl tip losses.

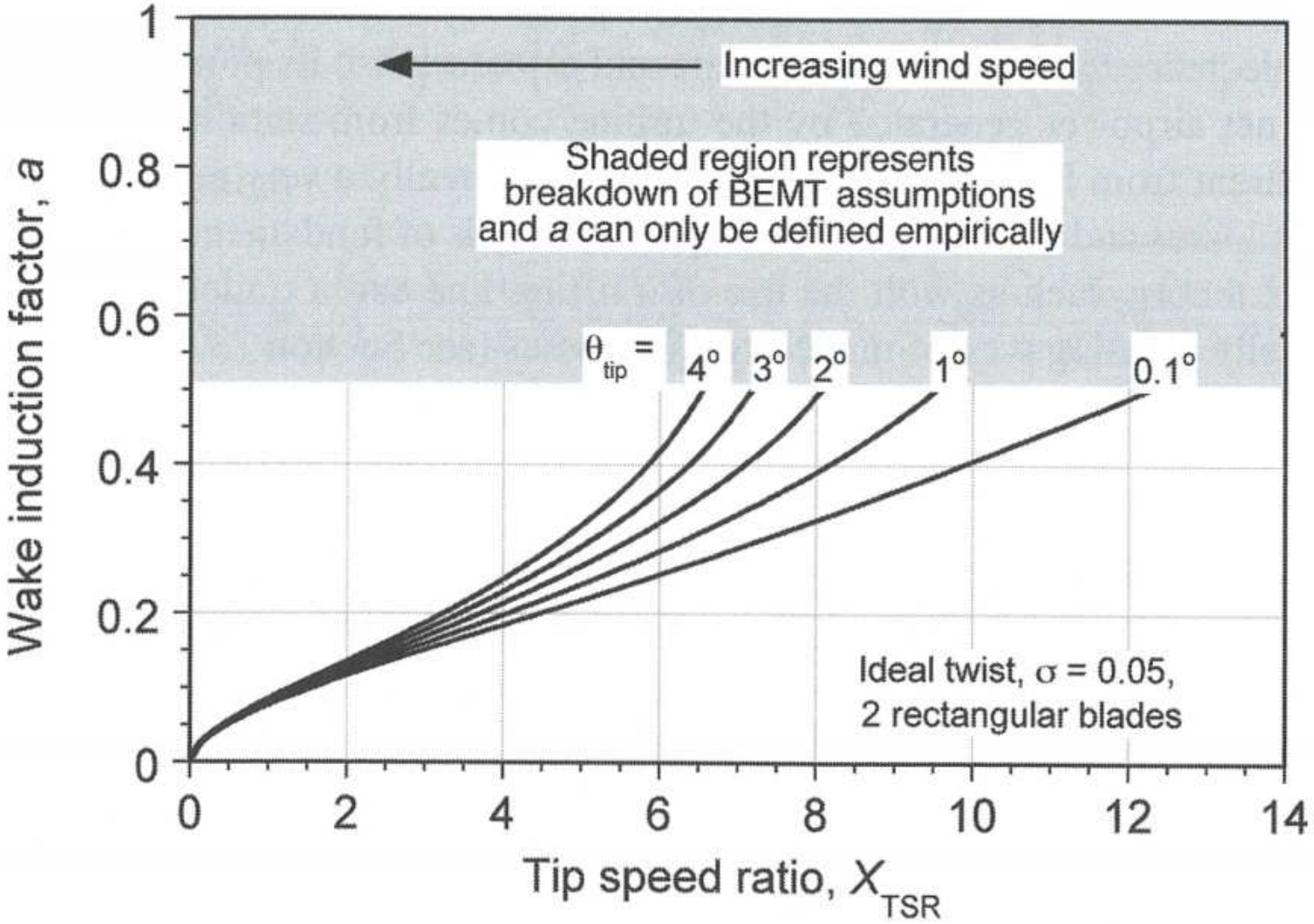

Figure 13.16 Variation of axial induction factor as a function of TSR for a wind turbine with ideally twisted blades giving uniform induction factor.

13.8.5 Effects of Stall

- Occurs at high speed (low X) and/or high blade pitch angles
- Can be incorporated in BEMT using a look-up table
- Stall causes power to drop more sharply with increasing wind speed
- Figure in next page shows results

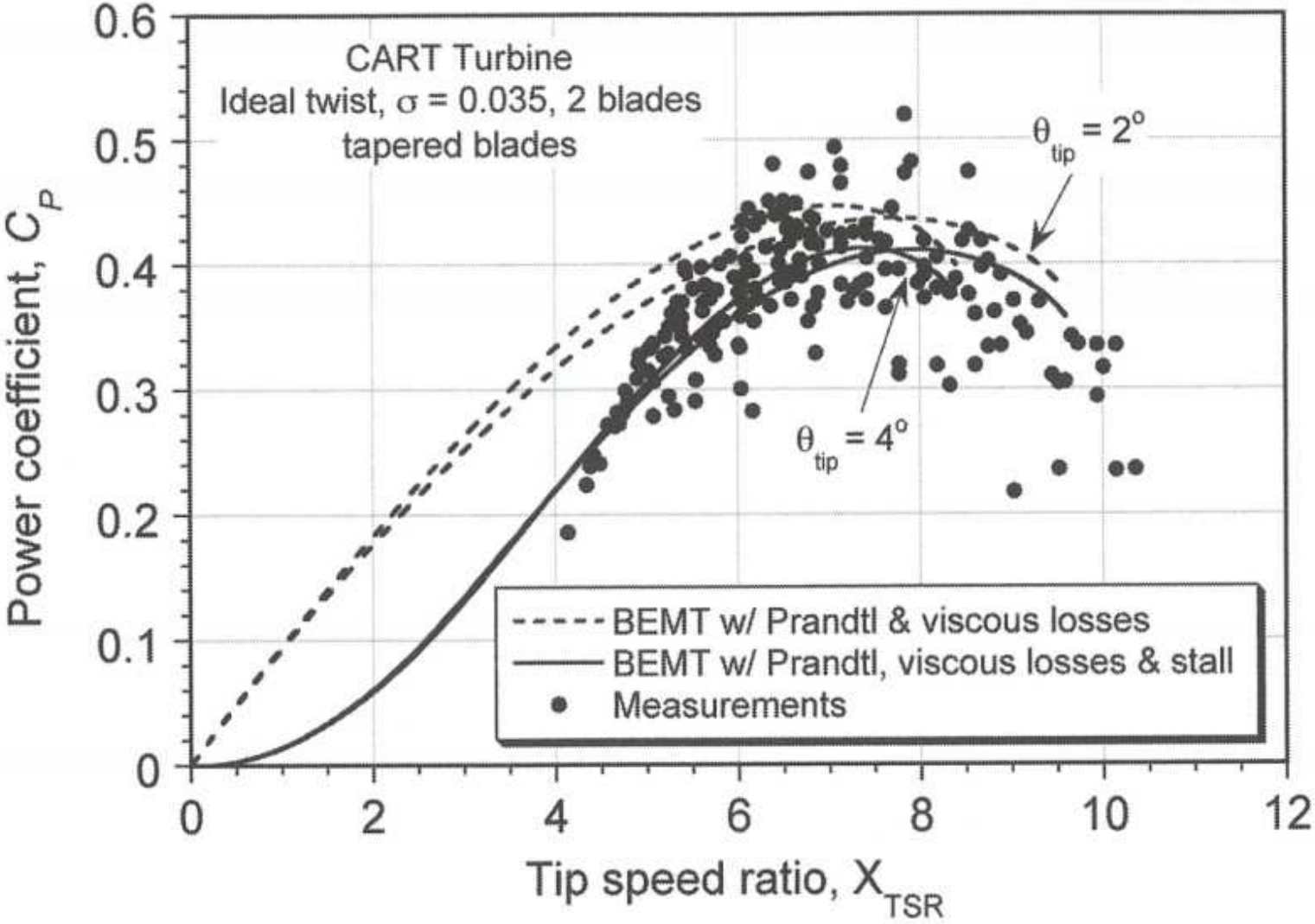

Figure 13.17 Turbine power output as a function of TSR showing the effects of blade stall. Data source: Measurements from two-bladed wind turbine, courtesy of NREL.

- Airfoils for Wind Turbines
  - Families of airfoils developed for wind turbines
  - NACA 4-digit, NASA LS-1 airfoils, NREL airfoils (see fig.)
  - Low Reynolds #s
    - Re # sensitivity, look up tables or equations
  - Sensitivity to surface roughness, see fig. - fig. 7.37
    - Increased drag, decreased C_{lmax}, “soft” stall
  - For variable pitches turbines high C_{lmax} is important (see also section 7.9)
    - Pitch control adjusts AoA for best energy extraction
  - For fixed pitch airfoils begin stall at low C_l values, but maintain the lift for a wide range of AoA (e.g. S809)
    - This trend carries over for unsteady conditions too.

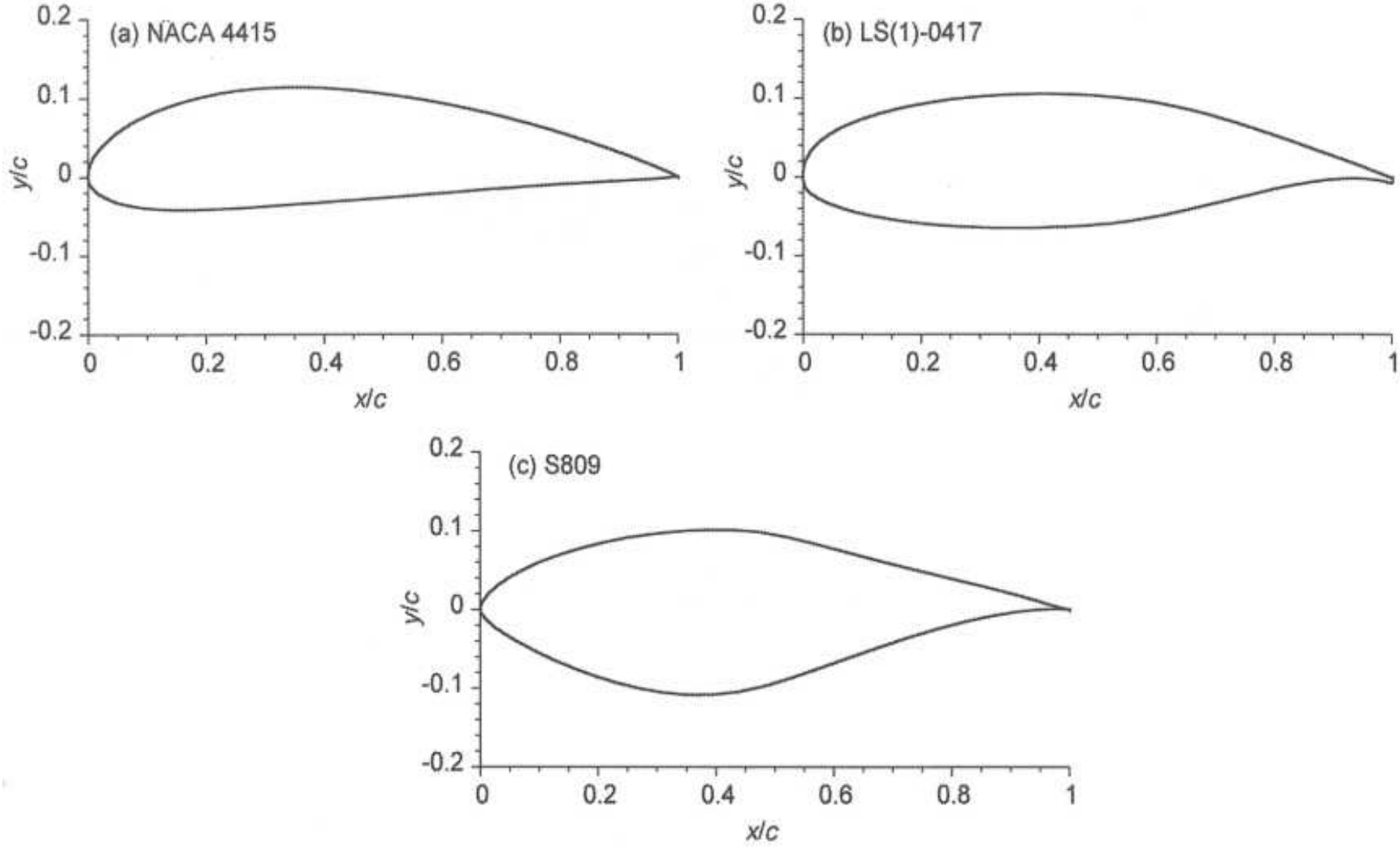

Figure 13.18 Examples of airfoil sections used for wind turbines: (a) NACA 4415. (b) LS(1)-0417. (c) NREL S809.

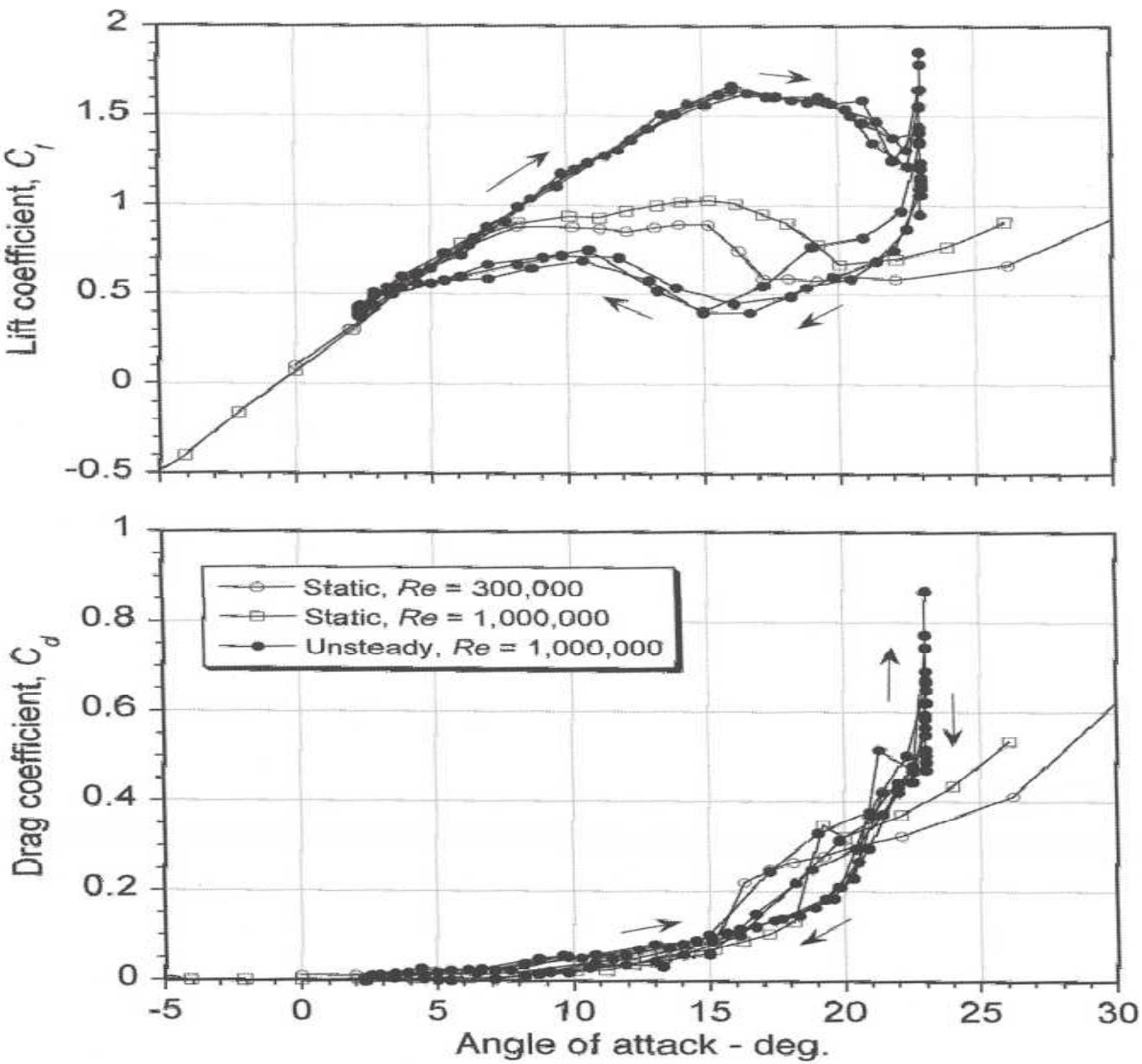

Figure 13.19 Lift and drag characteristics of the NREL S809 wind turbine airfoil under steady and unsteady conditions with dynamic stall ($\alpha = 10° + 10°\omega t$, $k = 0.077$). Data sources: Ramsay et al. (1995) and Hand et al. (2001).

13.10 Yawed Flow Operation

- Yaw misalignment to wind flow leads to skewed wake.
- Inflow gradient across the wind turbine
  - Strong // to the direction of the wake skew
  - Also in the other direction because of asymmetry of aerodynamic loads
- Vortex theory is needed (BEMT axisymmetric); or assume:

$$a_\gamma = a\left(1 + K_s(\gamma) r \sin\psi + K_c(\gamma) r \cos\psi\right) \qquad (13.63)$$

  - γ is the yaw angle
  - a_γ is the corrected value for a (induction ratio)
  - A good approach is to correct the value of a and iterate (momentum balances)
  - Ks and Kc can be found from inflow measurements, or
- where:

$$K_s = \tan(\chi/2) \qquad (13.64)$$

$$\chi = (0.6a + 1)\,\gamma \qquad (13.65)$$

- 13.11 Vortex Wake considerations
  - BEMT good preliminary predictions, insight into parameters (e.g. blade planform, twist)
  - Yaw is 3D→3D wake complicated structures (see next fig.)
    - Distortions may also be due wind gradient.
  - BEM modifications (e.g. using inflow models section 3.5.2)
  - Vortex methods (section 10.7)
    - incompressible potential flow vorticity concentrated in vortex filaments
    - vortex filament strengths induced velocities are obtained from Biot-Savart law
    - higher cost – more accurate.
  - Prescribed vortex: position specified apriori aided by experiments; steady-state
  - Free vortex: elements are allowed to convect freely
    - Thousands of elements needed (high cost), time accurate

Figure 13.20 Photograph of the vortical wake behind a horizontal axis wind turbine rendered visible using smoke injection. Notice the skewed wake resulting from the wind gradient and the effects of the tower shadow. Source: Photo courtesy of NREL.

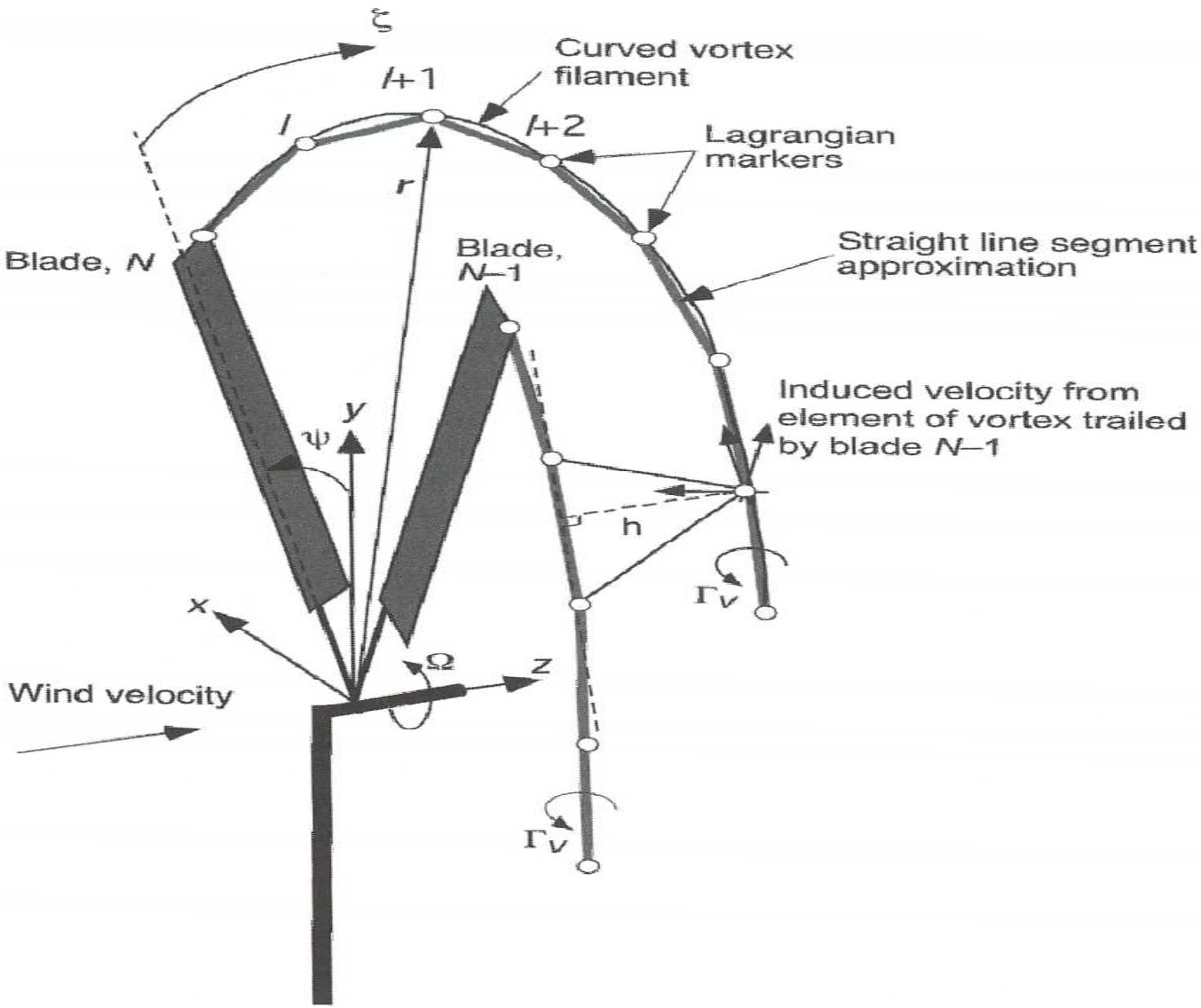

Figure 13.21 Modeling the downstream wake of a wind turbine using a free-vortex filament method, with vortices shown trailing from the tips of each blade.

- Time accurate predictions for a 2-bladed HAWT are shown in the next figure (13.22)
  - At high tip speed ratio (low wind speeds) vortex ring state (part a)
  - Lowering tip speed ratio: turbulent wake state (part b)
  - Lowering tip speeds ratio further: wake convers more quickly downstream
- C_P is shown next

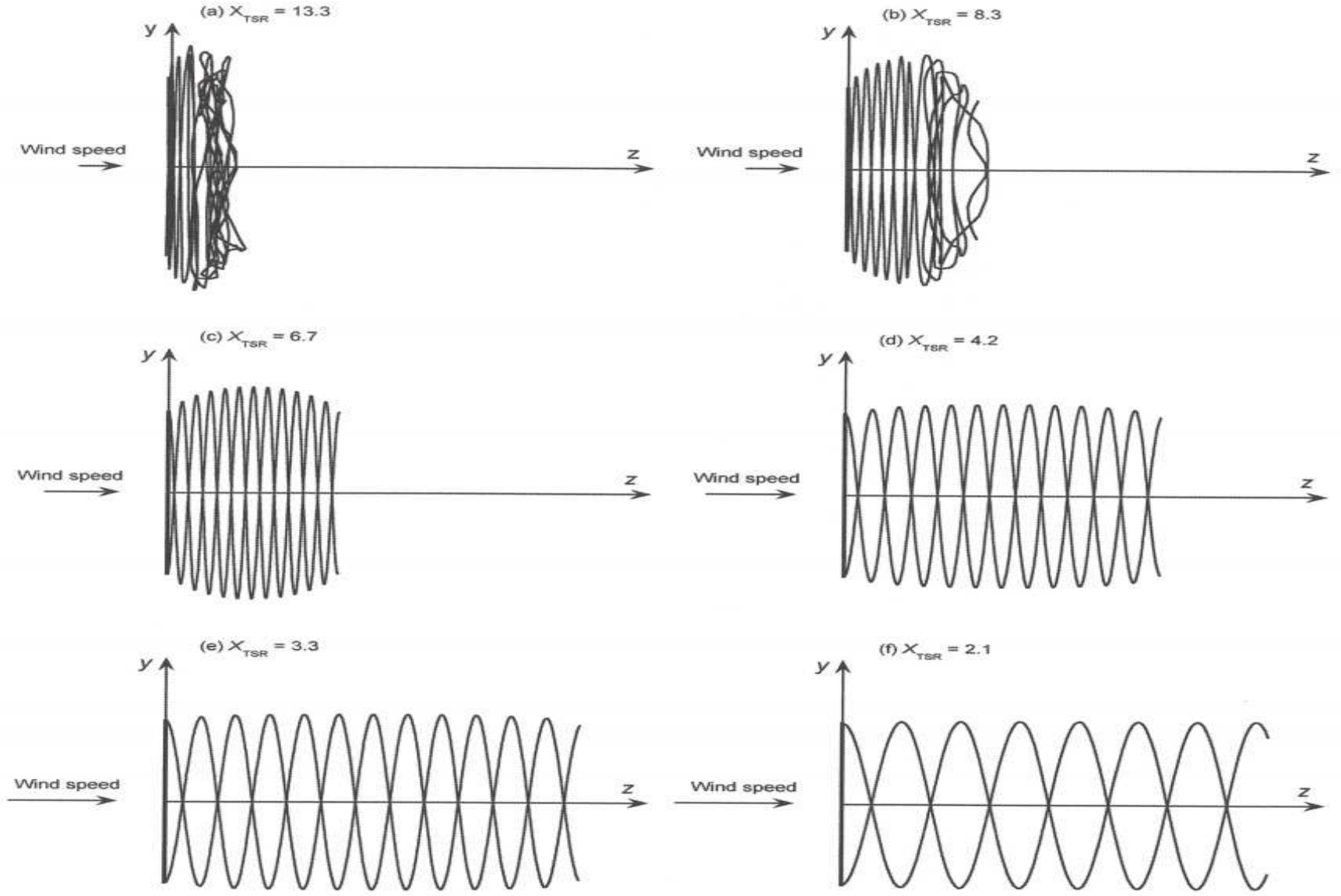

Figure 13.22 Predictions of the development of the vortex wake behind a wind turbine at various tip speed ratios using a FVM. Top views of wake: (a) $X_{TSR} = 13.3$, (b) $X_{TSR} = 8.3$, (c) $X_{TSR} = 6.7$, (d) $X_{TSR} = 4.2$, (e) $X_{TSR} = 3.3$, and (f) $X_{TSR} = 2.1$.

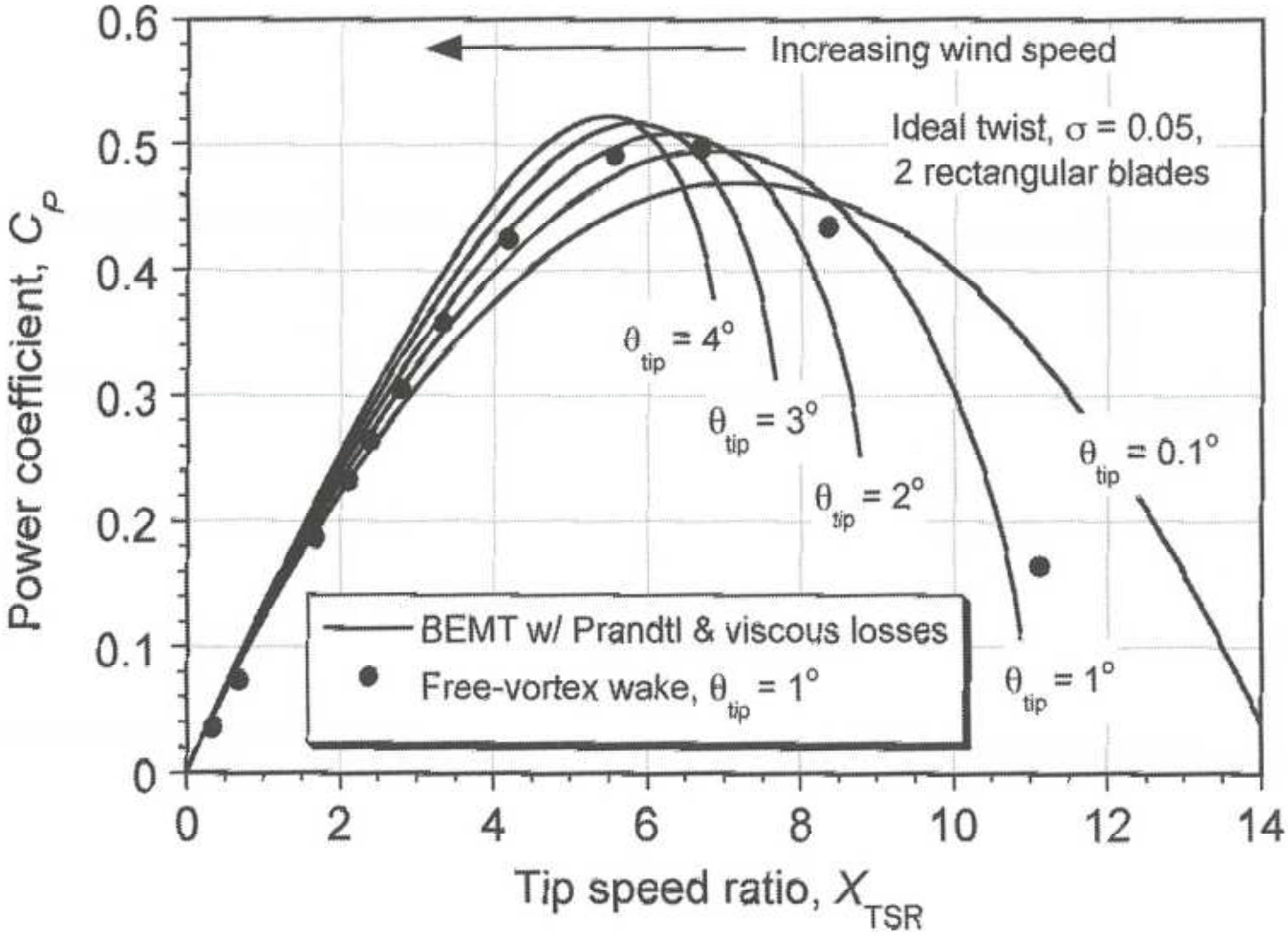

Figure 13.23 Power coefficient as a function of tip speed ratio using vortex wake and BEMT theories.

- Time-accurate calculations for 30^o yaw (after start with no yaw) are shown in the next figure.
  - Initially blades move into their own wake
  - After 10 revs periodic solution again

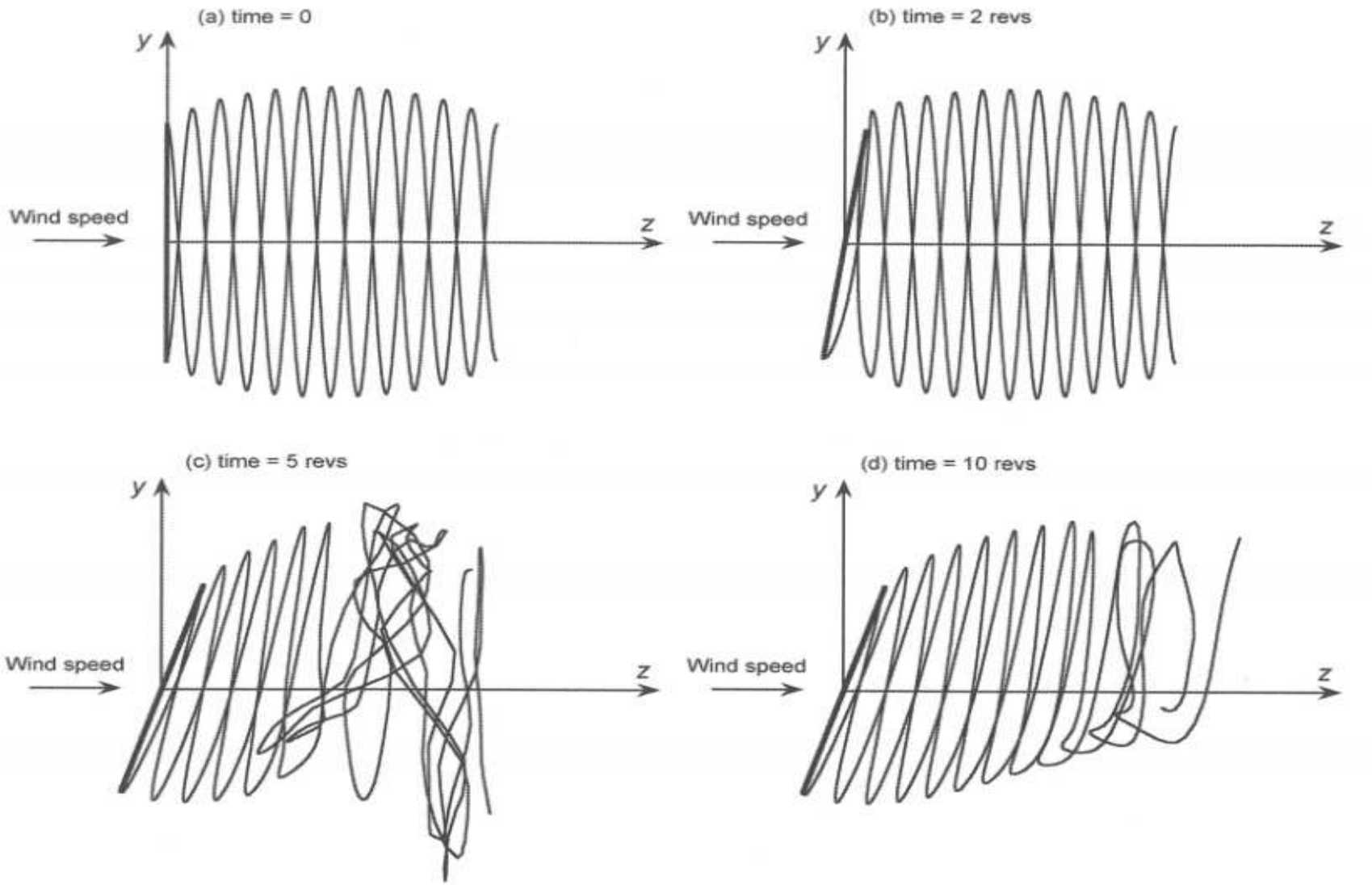

Figure 13.24 Free-vortex wake calculations of a three-bladed wind turbine yawing 30° out of wind. Top views of evolving wake: (a) Time = 0. (b) Time = 2 revs. (c) Time = 5 revs. (d) Time = 10 revs.

- Time history of Cp is shown next
  - Power drops 35% initially (cos3γ factor, see eq. 13.2)
  - Then equilibrium – some recovery
  - Dynamic inflow theory-section 10.9 (unsteady aerodynamic lag of the inflow over turbine disk in response to changes in blade pitch or turbine thrust)

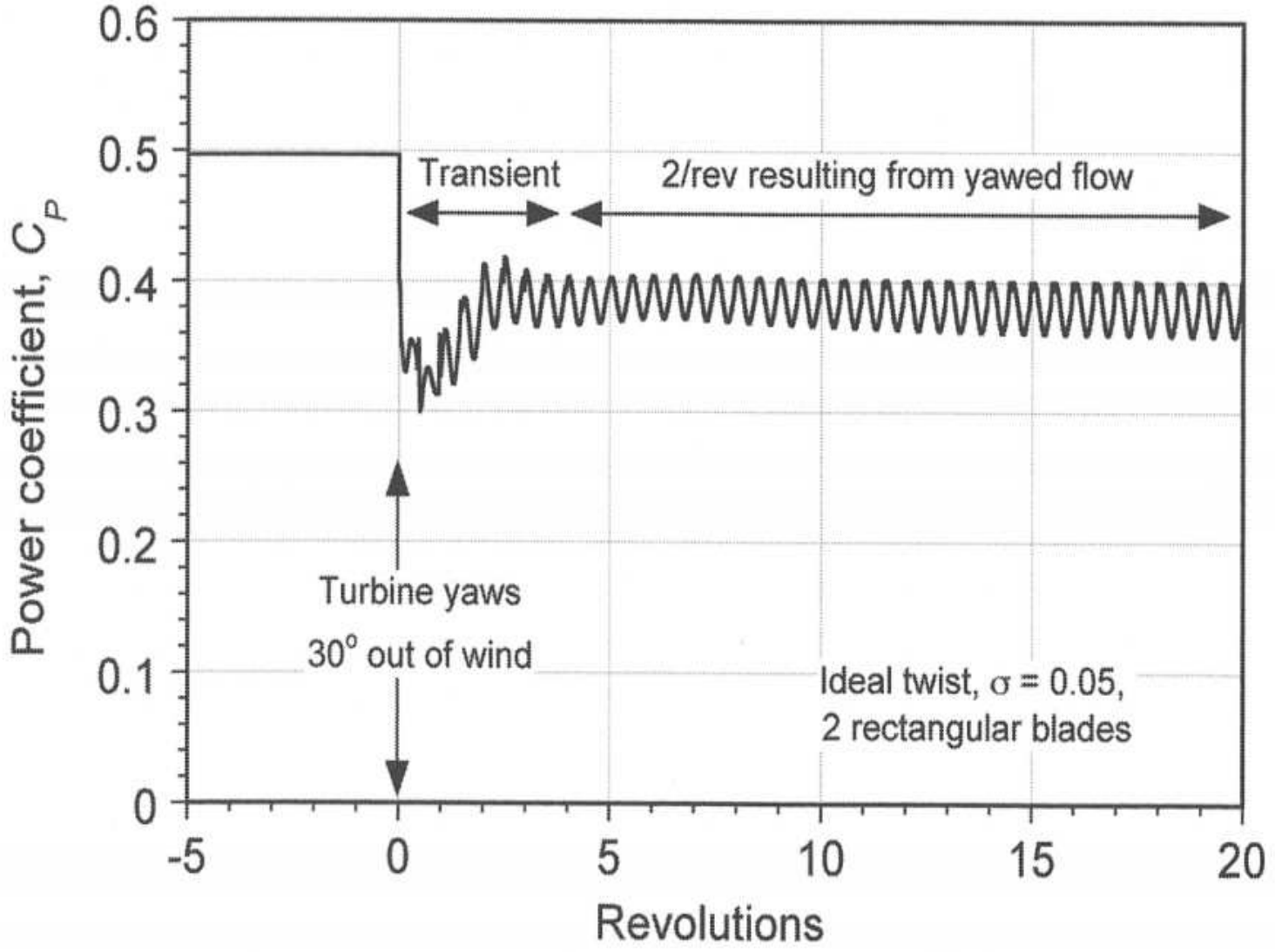

Figure 13.25 Power coefficient as a function of time for the condition when the turbine is suddenly yawed out of the wind.

13.12 Unsteady Aerodynamic Effects on Wind Turbines

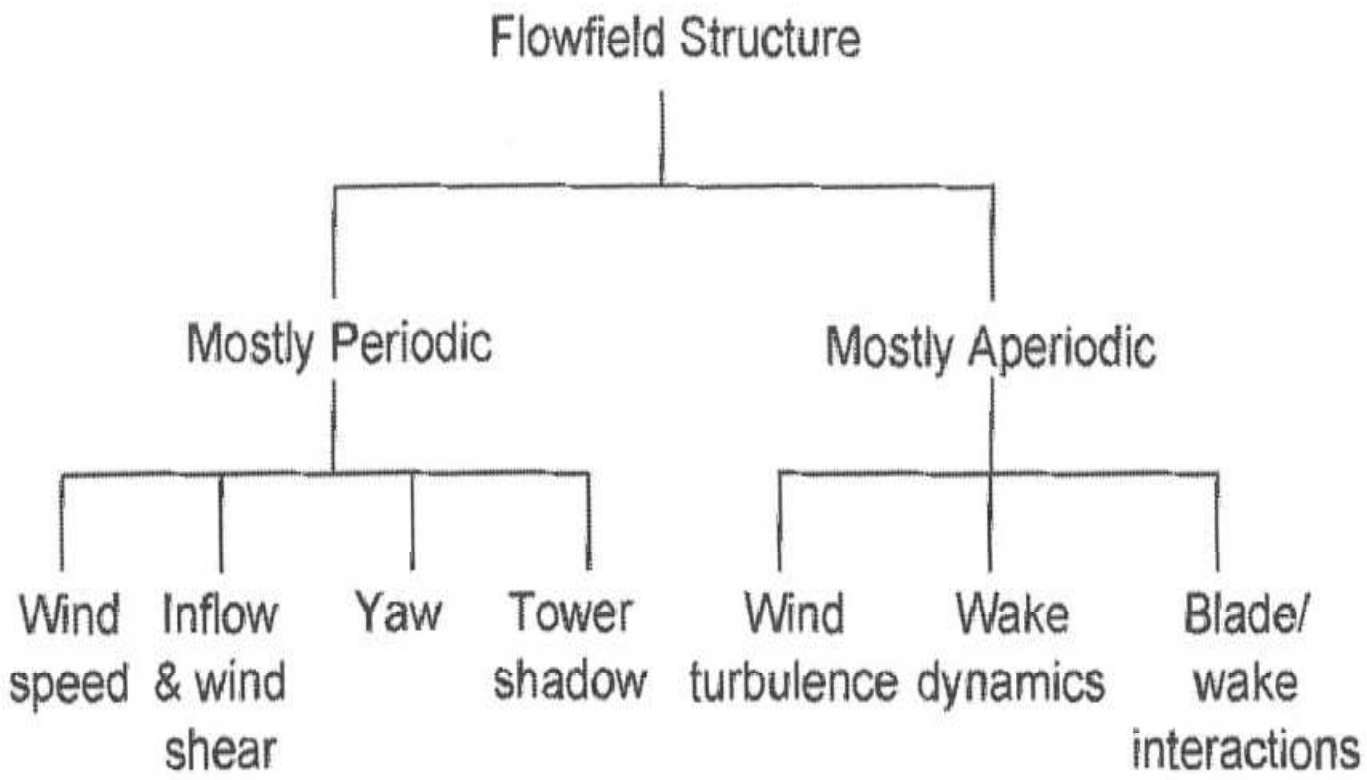

Figure 13.26 Summary of the various aerodynamic sources that contribute to the airloads on a wind turbine.

- Yaw misalignment is important
- Blade flapping effects
- Due to low speeds (20rpm for large 800 rpm for small turbines)
  - relatively low noise
  - Significant changes in AoA due to changes in wind speed
  - Reduced frequencies can be high
- Reduced frequency for yaw

$$k = \frac{\Omega c}{2(\Omega R r + V_\infty \sin\gamma)} = \left(\frac{1}{r + \sin\gamma / X_{\text{TSR}}}\right)\frac{c}{2R} \qquad (13.66)$$

- Typical value R/c=10, k~0.1 (for K<0.05 ~quasi-steady); Specific effects are:

- 1. Varying wind speed
  - Modest wind fluctuations change AoA significantly.
    - output transients
    - unsteady forces
    - Lag of inflow (wake adjustments ~ 10 revs
- 2. Velocity gradients in the wind (fig. 13.20)
  - Nonuniform AoA - unsteadiness
- 3. Non-steady velocity fluctuations in yawed flow
  - Large excursions from axial flow
    - Significant unsteady effects
    - Cannot assume small disturbances
- 4. Unsteady wake induction effect
  - Lag in inflow development

- 5. Local sweep effects
  - Local sweep angle can be large when turbine is yawed
  - Stall might occur
- 6. Tower shadow effects
  - Important for downstream and upstream turbines
  - k~0.2 (high) – airfoil with gust

- 13.12.1 Tower Shadow
  - Can be seen in fig. 13.20
  - Velocity deficiency (up to 30%) approaching turbine disk
  - 2-D airfoil, with V=1, and disturbance (normal to the chord)

$$w=0.08+0.02\cos(5\psi),\ 144^{o}\leq\psi\leq216^{o}$$

  - Fig. below shows difference of unsteady and quasi-steady approaches

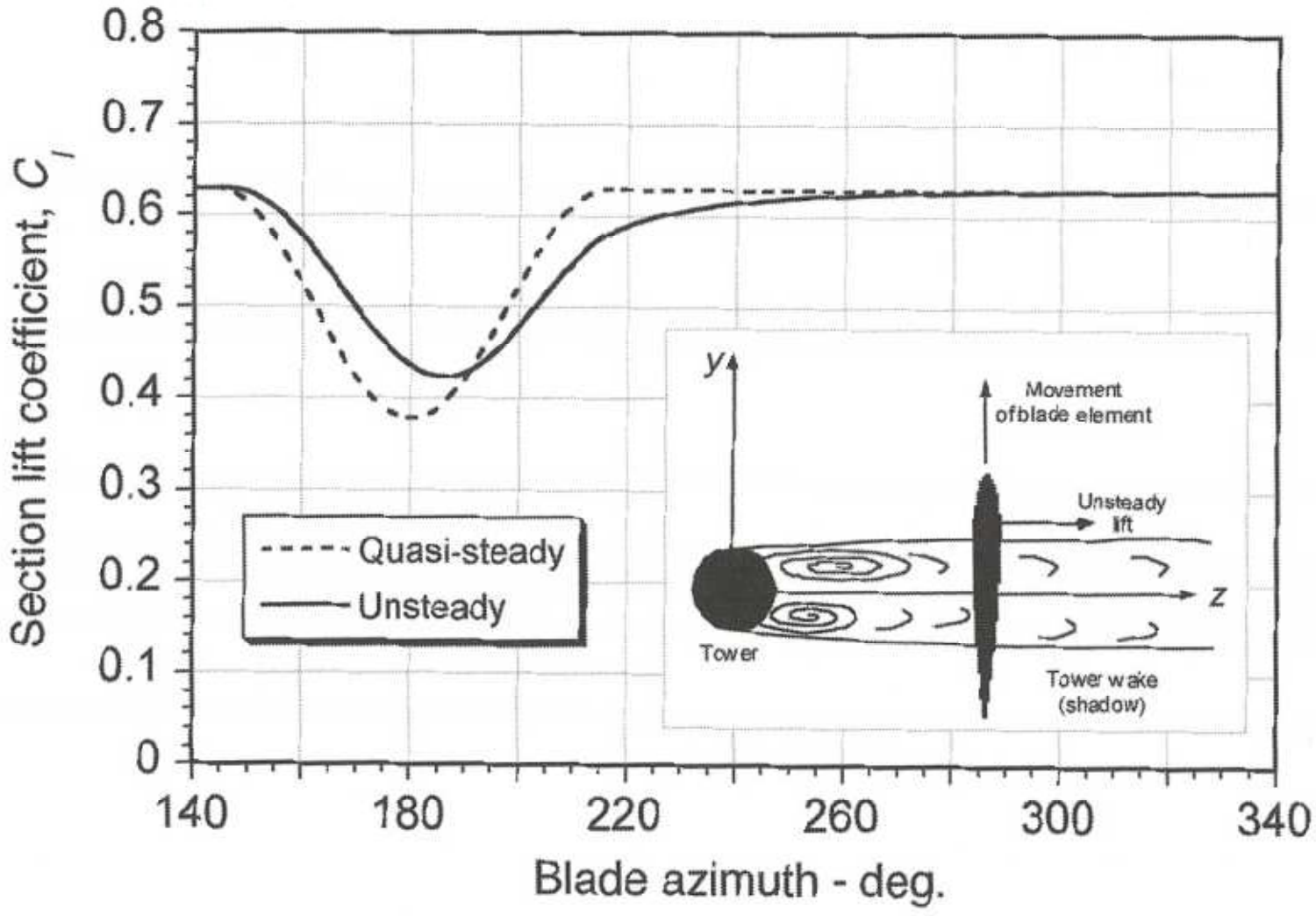

Figure 13.27 Prediction of the unsteady lift during a simulated tower shadow encounter using 2-D unsteady airfoil theory.

13.12.2 Dynamic Stall and Stall Delay

- Stall leads to large unsteady airloads (can cause structurar damage)
- Unsteady airloads exist even without stall; unsteady flow without stall needs to be known first
- Semi-empirical models for stall (e.g. Leishman Beddoes)
- Figure below shows that stalls creates a lot of turbulence
- Stall effects
  - Unsteady pressure gradient reduction effects delay in 3-D boundary layer development
  - Coupled influences of centrifugal and Coriolis effects on the boundary layer in rotating flow
- Coriolis acceleration forces can act to alleviate adverse pressure gradients and may delay the onset of flow separation and stall

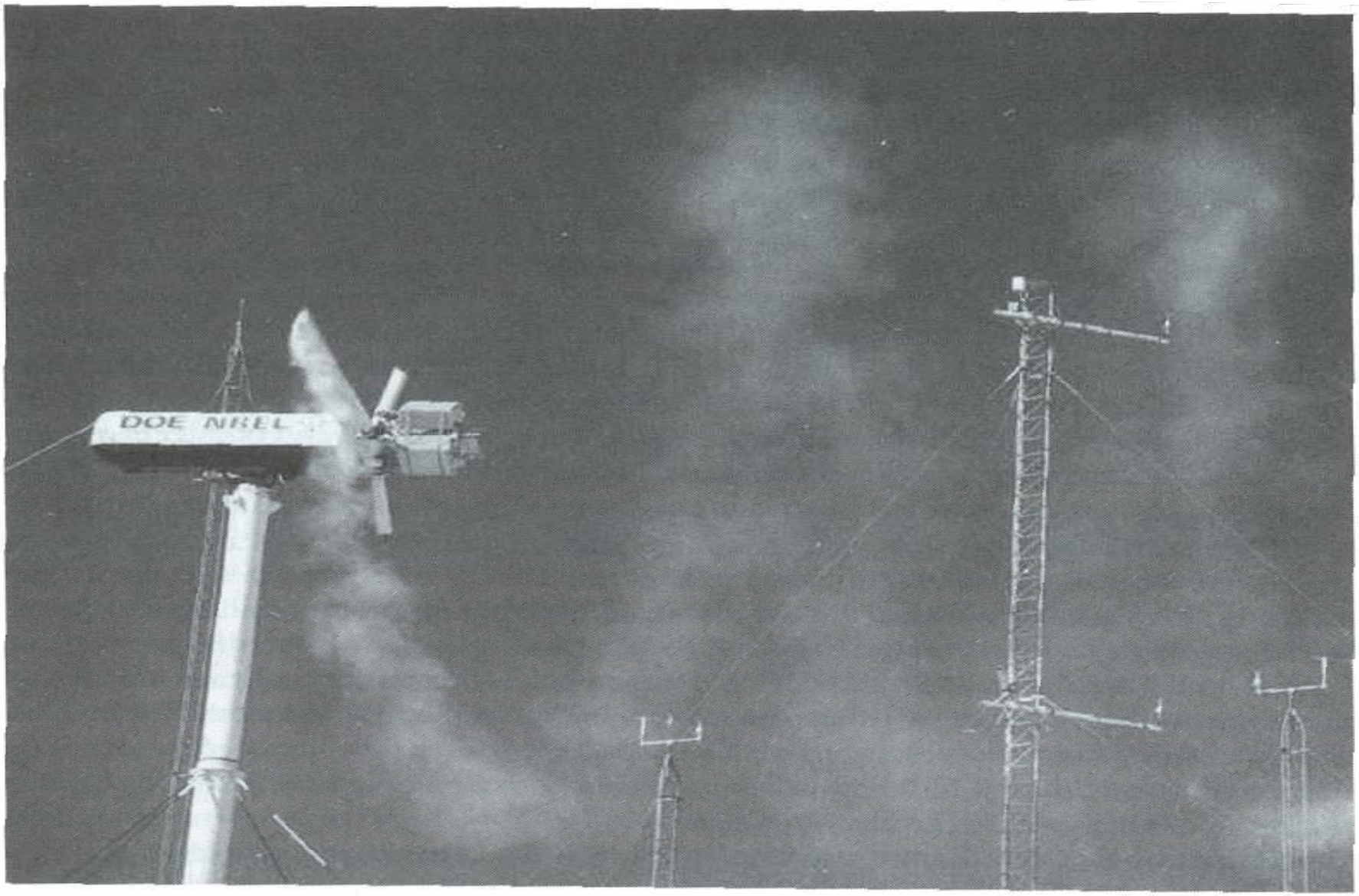

Figure 13.28 The onset of stall on the turbine produces highly nonlinear aerodynamic loads and a turbulent wake structure. Source: Photo courtesy of NREL.

- The modified boundary layer equations are

$$\frac{\partial u}{\partial x} + \frac{\partial w}{\partial z} = 0 \quad \text{(continuity)} \tag{13.67}$$

$$u\frac{\partial u}{\partial x} + v\frac{\partial u}{\partial z} - \Omega^2 x = -\frac{1}{\rho}\frac{\partial p}{\partial x} + \nu\frac{\partial^2 u}{\partial z^2} \quad (x \text{ momentum}) \tag{13.68}$$

$$u\frac{\partial v}{\partial x} + w\frac{\partial v}{\partial z} + 2\Omega u - \Omega^2 x = -\frac{1}{\rho}\frac{\partial p}{\partial y} + \nu\frac{\partial^2 v}{\partial z^2} \quad (y \text{ momentum}) \tag{13.69}$$

$$-\frac{\partial p}{\partial z} = 0 \quad \text{(pressure gradient normal to surface)} \tag{13.70}$$

- x: chordwise, y: spanwise, z normal to the blade
- W2x terms: centipetal accelerations
- 2Wu: Corriolis acceleration

- Effects of radial flow more important in wind turbine blades (higher values of Cl)
- There is some experimental and CFD evidence (stall delay due to 3D effects)

13.13 Advanced Aerodynamic Modeling Issues

- BEMT + structural dynamic analysis can be used
- CFD has some problems to overcome: separation (dynamic stall), vortical wake (difficulty preserving concentrated vorticity)